Deposition of Aluminium Oxide Modified Core-shell Silica Particles onto Silica Surfaces

A thesis submitted to the University of Manchester for the degree of Master of Philosophy in the Faculty of Engineering and Physical Sciences

2010

Caroline Alexandra Hall

School of Physics and Astronomy

Contents

Word Count 16422

Tables and Figures

Chapter 2

Chapter 3

Chapter 4

Abstract

Modification of surfaces is of great interest to fundamental research and industrial application. Inorganic particles such as silica are of direct relevance to home and personal care industry. Although particles already enjoy a wide range of applications, there are ongoing studies to develop new applications based on novel surface functionalities and particle interactions with other particles and substrate surfaces. Manipulation of surface charge properties is one of foremost handles in tuning particle system behaviour.

In this study, the deposition of modified core-shell silica particles (Ludox CL) onto a flat silica surface was studied with increasing concentration of the particles in the dispersion and the results were compared with bare silica particles (Ludox HS). Ludox CL particles were silica spheres with their surfaces modified by reacting with aluminium chloride to form an outer coating of aluminium oxide. The modified silica particles were first characterised under different solvent conditions. Measurements of particle size and surface charge were performed and tracked with changes in pH and electrolyte concentration. Particle deposition onto silica surface was then investigated at increasing concentrations under changing pH and electrolyte conditions. The morphology and amount of deposited material were observed and relevant techniques were used in order to shed light on the observed phenomena. In aqueous solution, the coated silica particles manifested the surface properties of colloidal alumina with a high cationic Zeta potential at low pH values and an isoelectric point around pH 8.5-9. Increasing pH caused a steady process of leaching of aluminium ions, leading to preferential adsorption of the solvated cations to anionic silica surfaces and thus impeding the deposition of silica particles. As a result of leaching of aluminium ions, the silica substrate was modified and this in turn influenced the morphology of the deposited clusters.

Declaration

No portion of the work referred to in this thesis has been submitted in support of an application for another degree or qualification of this or any other university or other institute of learning.

Copyright Statement

(i) The author of this thesis (including any appendices and /or schedules to this thesis) owns certain copyright or related rights in it (the "Copyright") and s/he has given The University of Manchester certain rights to use such Copyright, including for administrative purposes.

(ii) Copies of this thesis, either in full or in extracts and whether in hard or electronic copy, may be made only in accordance with the Copyright, Designs and Patents Act 1988 (as amended) and regulations issued under it or, where appropriate, in accordance with licensing agreements which the University has from time to time. This page must form part of any such copies made.

(iii) The ownership of certain Copyright, patents, designs, trade marks and other intellectual property (the "Intellectual Property") and any reproductions of copyright works in the thesis, for example graphs and tables ("Reproductions"), which may be described in this thesis, may not be owned by the other and may be owned by third parties. Such Intellectual Property and Reproductions cannot and must not be made available for use without the prior written permission of the owner(s) of the relevant Intellectual Property and/or Reproductions.

(iv) Further information on the conditions under which disclosure, publication and commercialisation of this thesis, the Copyright and any Intellectual Property and/or Reproductions described in it may take place is available in the University IP Policy (see http://www.campus.manchester.ac.uk/medialibrary/policies/intellectual-property.pdf), in any relevant Thesis restriction declarations deposited in the University Library, The University Library's regulations (see http://www.manchester.ac.uk/library/aboutus/regulations) and in The University's policy on presentation of Theses

Acknowledgements

Acknowledgement must go to my local supervisor Jordan Petkov and my University supervisor Jian Lu who both, along with Ian Tucker at Unilever Research, helped enormously with their advice and support during the writing of this thesis. My thanks, for their expertise and valuable input into the experimental design and data interpretation during our regular project reviews.

Thanks to Unilever Research for the sponsorship of this study.

Thanks to my project leaders at Unilever Research who gave me the time to complete this thesis.

1 Introduction and Literature Review

1.1 Introduction

Modification of surfaces is of great interest to both fundamental study and industrial application, ranging from understanding process engineering[1], delivery of actives[2] and creating super coatings[3] to simple cleaning of surfaces or changing the sensory properties of hair and skin. It is of strong interest to the home and personal care business to monitor how the deposition of particles changes the friction and lubrication behaviour of the surfaces which can lead to new business opportunities. Hence this work was undertaken to look at how commercially available silica and modified silica were deposited onto surfaces and the morphologies created subsequently.

1.2 Literature Review

Silica has been extensively studied in a variety of ways. Since synthesis of relatively monodispersed particles was first achieved [4,5] understanding the mechanisms of particle formation and how to modify those conditions have been investigated. [6,7] Particles have also been utilised to stabilise emulsions [8], act as templates [9, 10, 11] and modify surfaces [3]. Much has been done in preparing monodispersed silica particles and how to control the particle morphology and size [12-14] with the effects of surfactants on particle synthesis also examined [15-17]. Hybrid silica materials have been studied where the silica surface is modified using silanes carrying different functional groups [18] or the silica and silane are co-synthesised to produce different morphologies and chemical properties [19-21]. Further modifications of silica surfaces can be performed using standard polymers [22-26] and surfactants [27, 28] to more exotic shell cross-linked micelles [29,30] and liquid crystalline nanoparticles [31] not forgetting biomolecules [32]. These all find applications in coatings, catalysis, chromatography and bio-assays [33-35] and are of interest for assembly of silica nanoparticles onto surfaces [36] for applications such as superhydrophilicity [37], chemical sensors [38] or photonic crystals [39]. Silica particles can also be engineered as agents for drug delivery [40].

Silicas are widely used as models to understand colloidal particle behaviour [41, 42]. Light scattering and SEM/TEM are utilised to identify changes in particle size and morphology during synthesis [17, 19, 21] whilst electrokinetic measurements (electrophoresis and electroacoustics [43]) are commonly used to probe effects of particle density [44] and interaction forces [45] such as depletion flocculation that lead to instability in solution [46, 47]. Sedimentation or rheology is often observed as well to compliment the electrokinetic measurement [47, 48] and understand aggregation rates and morphology [49]. Deposition of silica particles onto surfaces has previously been probed using quartz crystal microbalance [50], ellipsometry [36] and SEM whilst surface force measurements [51, 48] can be used to look at the specific interactions between a particle and a surface. Most studies onto surfaces have been for use in the coatings industry [52-55].

Aluminium oxide and titanium oxide are other colloidal particles that have been used extensively to probe colloidal stability through studies of coagulation and surface charge [56, 57] and the effects of electrolytes and polymers[48, 58]. Aluminium oxide is similar to silica, in that the surface charges are highly influenced by the solution chemistry and often driven by pH. This can lead to instability of the colloidal material and also influence the deposition behaviour as the surface charges on the particles change.

Inorganic particles are of particular interest in the home and personal care industry. Titanium dioxide and zinc oxide are commonly used in sunscreen formulations whilst both silica and alumina are used as abrasives in toothpastes. Aluminium salts are used as active components in deodorants and anti-perspirants and clays are employed to modify viscosity. The cosmetics industry makes use of clays in powder bases and masks while iron oxides are extensively used to modify colour, glitter and shine for eye-shadows, lipsticks etc. Although they already have a wide range of uses, inorganic particles have the ability to act as a template or be modified and this is developing all the time. These particles can then be used in a variety of new ways thus employing potential new functionalities.

1.3 Current Study

In this study, the deposition of a type of modified core-shell silica particles onto flat silica surface was studied with increasing concentration of the particles in the dispersion. These particles (Ludox CL) are silica particles that have been surface modified by reacting with aluminium chloride to leave a coating of aluminium oxide attached to the silica. The equivalent non-modified silica was also studied as a control. Of interest was the behaviour of the particles as they deposited onto a solid hydrophilic substrate and the morphology formed upon that surface. This knowledge could then be used to drive changes in surface properties and give required benefits for particles on biological substrates.

The standard and modified silica particles were first studied in the dispersion to determine their characteristics. Measurements of particle size and surface charge were performed and tracked with changes in pH and electrolyte concentration. Particle deposition onto silica surface was then probed at increasing concentrations under variable pH and electrolyte conditions. The morphology and amount of deposited material were observed and more techniques were used in order to shed light on the mechanistic processes.

1.4 References

1. Behringer R.P., *Int. J. Bifucation Chaos* **7**, 963 (1997)
2. Wooley K.L., *J Polymer Sci, Polymer Chem* **38**, 1397 (2000)
3. Liu X., He J., *J Colloid Interface Sci* **314**, 341 (2007)
4. Stober W., Fink A., *J Colloid Interface Sci* **26**, 62 (1968)
5. Matijevic E., *Langmuir* **10**, 8 (1994)
6. Van Blaaderen A., Van Geest J., Vrij A., *J Colloid Interface Sci* **154**, 2 (1992)
7. Van Blaaderen A., Vrij A., *J Colloid Interface Sci* **156**, 1 (1993)
8. Hunter T.N., Pugh R.J., Franks G.V., Jameson G.J., *Advances in Colloid and Interface Sci* **137**, 57 (2008)
9. Lihitkar N.B. et al, *J Colloid Interface Sci* **314**, 310 (2007)
10. Shimura N., Ogawa M., *J Colloid Interface Sci* **312**, 311 (2007)
11. Ohkubo T., Ogura T., Sakai H., Masahiko A., *J Colloid Interface Sci* **312**, 42 (2007)
12. Tan C.G., Bowen B.D., Epstein N., *J Colloid Interface Sci* **118**, 290 (1987)
13. Wang W., Gu B., Liang L., Hamilton W.A., *J Phys Chem B* **107**, 3400 (2003)
14. Wang W., Gu B., Liang L., Hamilton W.A., *J Phys Chem B* **107**, 12113 (2003)
15. Wang W., Gu B., Liang L., Hamilton W.A., *J Phys Chem B* **108**, 17477 (2004)
16. Portet F., Desbene P.L., Treiner C., *J Colloid Interface Sci* **208**, 415 (1998)
17. Wang W., Gu B., Liang L., *J Colloid Interface Sci* **313**, 169 (2007)
18. Vansant E.F., Van der Voort P., Vrancken K.C., Characterisation and Chemical Modification of the Silica Surface, Elsevier, Amsterdam, 1995
19. Bambilla R., Pires G.P., dos Santos J.H.Z., Lacerda Miranda M.S., *J Colloid and Interface Sci* **312**, 326 (2007)
20. Miller C.R., Vogel R., Surawski P.P.T., Jack K.S., Corrie S.R., Trau M., *Langmuir* **21**, 9733 (2005)
21. Vogel R. et al, *J Colloid Interface Sci* **310**, 144 (2007)
22. Mubarekyan E., Santore M.M., *Macromolecules* **34**, 4978 (2001)
23. Huang Y., Santore M.M., *Langmuir* **18**, 2158 (2002)
24. Shin Y.W., Roberts J.E., Santore M.J., *J Colloid Interface Sci* **244**, 190 (2001)
25. Shin Y.W., Roberts J.E., Santore M.J., *Macromolecules* **35**, 4090 (2002)

26. McNamee et al, *Colloids and Interfaces A: Physiochem Eng Aspects* **193**, 175 (2001)
27. Forland G.M., Blokhus A.M., *J Colloid Interface Sci* **310**, 431 (2007)
28. La Mesa C. et al, *J Phys Chem C* **112**, 12142 (2008)
29. Pilon L.N., Armes S.P., Findlay P., Rannard S.P., *Langmuir* **21**, 3808 (2005)
30. Pilon L.N., Armes S.P., Findlay P., Rannard S.P., *European Polymer Journal* **42**, 1487 (2006)
31. Vandoolaeghe P., Campbell R.A., Rennie A.R., Nylander T., *J Phys Chem C* **113**, 4483 (2009)
32. Parida S.K. et al, *Advances in Colloid and Interface Sci* **121**, 77 (2006)
33. Chen S.W., You B., Zhou S.X. et al, *J Applied Polymer Sci* **112**, 6 (2009)
34. Zhoa W.A., Pacard E., Chaix-Bauvais C. et al, *Colloids and Surfaces A:Physiochem. and Eng. Aspects* **339**, 1-3 (2009)
35. D'Orazio G. Fanali S., *J Separation Sci*i **31**, 14 (2008)
36. An Y., Chen M., Xue Q., Liu W., *J Colloid Interface Sci* **311**, 507 (2007)
37. Cebecci F.C., Wu Z., Zhai L., Cohen R.E., Rubner M.F., *Langmuir* **22**, 2856 (2006)
38. Rampazzo E., Brasola E., Marcuz S., Mancin F., Tecilla P., Tonellato U., *J Mater Chem* **15**, 2687 (2005)
39. Toader O., John S., *Science* **292**, 1133 (2001)
40. Rigby S.P., Fairhead M., van der Walle C.F., *Current Pharmaceutical Design* **14**, 1821 (2008)
41. Matijevic E., *J Colloid Interface Sci* **43**, 2 (1973)
42. Aronson M.P., Petko M.F., Princen H.M., *J Colloid Interface Sci* **65**, 2 (1978)
43. James M., Hunter R.J., O'Brien R.W., *Langmuir* **8**, 420 (1992)
44. Reiber H. et al, *J Colloid Interface Sci* **309**, 315 (2007)
45. McNamee C.E. et al, *Langmuir* **17**, 6220 (2001)
46. Snowden M.J., Williams P.A., Garvey M.J., Robb I.D., *J Colloid Interface Sci* **166**, 160 (1994)
47. Allan G.C., Garvey M.J., Goodwin J.W., Hughes R.W., MacMillan R., Vincent B., Modern Aspects of Colloidal Dispersions, Kluwer Academic Publishers, Netherlands, 1998

48. Singh B.P., Menchavez R., Takai C., Fuji M., Takahashi M., *J Colloid Interface Sci* **291**, 181 (2005)
49. Dunleavy-Routh R., Vincent B., *J Colloid Interface Sci* **309**, 119 (2007)
50. Krozer A., Nordin S., Kasemo B., *J Colloid Interface Sci* **176**, 479 (1995)
51. Biggs S., Cain R., Page N.W., *J Colloid Interface Sci* **232**, 133 (2000)
52. Nagy L.N., Abraham N., Sepsi O., et al *Langmuir* **24**, 21 (2008)
53. Perelaer J., Smith P.J., Hendricks C.E., et al *Soft Matter* **4**, 5 (2008)
54. Helmecke O., Menneking C., Behrens P., et al *Colloid and Polymer Science* **286**, 3 (2008)
55. Tao M., Zhou W.D., Yang H.J., et al, *Applied Physics Letters* **91**, 8 (2007)
56. Wiese G.R., Healy T.W., *J Colloid Interface Sci* **51**, 3 (1975)
57. Wang X.H., Hirata Y., *J Ceramic Processing Research* **1**, 1 (2000)
58. Sprycha R., *J Colloid Interface Sci* **127**, 1 (1989)

2 Experimental - Theory

2.1 Photon Correlation Spectroscopy

2.1.1 Principles

Photon correlation spectroscopy, PCS, is concerned with the measurement of particle size[1], mostly in the size range 1-1000 nm. It probes the timescale associated with the movement of particles due to Brownian motion. For a system of particles that are smaller than the wavelength of light, as the photon transverses the particle the electromagnetic wave senses a change in dielectric property. As the particle is smaller than the wavelength there can be no coherent scattering events and the interconversion of excess energy results in the emission of a secondary dipolar field which emits radially about the particle. For a dilute dispersion of particles, the interference of these dipolar fields results in a fine interference pattern known as a “Speckle pattern” when viewed in far-field. As these particles are not frozen in space, the speckle intensity at any point varies at the frequency of 1/diffusion time for the particles. Thus when a particle moves along the Q vector of the radiation, the intensity in far-field fluctuates with this periodicity and using correlation based methods, it is possible to extract this characteristic timescale. Larger particles have slower Brownian motion whilst smaller particles are bombarded further and more rapidly by solvent molecules, hence the fluctuations in the light intensity are more rapid for small particles. However, there exists a fundamental limit for small and large particles. The large particle limit is due to slow particle motion where the particle matches the rate of diffusion due to the convection in the sample. This is typically in the region of 3 microns upwards but is also dependent upon the size of the vessel being utilised and particle density. For small particles, the limit is due to both the correlator and the optical resolution. Enough particles need to be present in solution to scatter otherwise there is no signal but if they are moving too fast, they can reach the limit of the acquisition speed of the detector.

In order to interpret these fluctuations, a digital auto-correlator is used. This is a signal comparator and is designed to measure the degrees of similarity between 2 signals or one signal with itself over time. If a signal is compared with itself at two different time

points, then for a random process such as diffusion, the fluctuating signal intensities will not be related in any way. However, if the signal intensity at some arbitrary time = t is compared to itself a very small time later, t+δt, then there will be a strong correlation. If the signal at t is then compared to the signal at t+2δt, the correlation will be less strong and will continue to reduce with time. The period of time δt is usually very small and is known as the sample time. For a logarithmic correlator, this unit of time is increased by the power of e instead of 2, 3, etc. Perfect correlation is indicated by unity (1.00) where the signal intensity is compared with itself at time t, whilst no correlation is indicated by zero (0.00) and this is recorded in the instrument correlation function. This gives a lot of information about the measured sample as large particles, with a slowly fluctuating signal, will produce a good correlation for a longer period than smaller particles with their rapid movement. Figure 2.1 shows simulated correlation functions produced for large particles (a) and smaller particles (b).

This can be modelled by an exponential of the form:

$$g(\tau) \approx A.\exp-(\mathrm{B}t)+\mathrm{K} \qquad (2.1)$$

where $g(\tau)$ is the correlation function, A is the intercept and B is the time constant of the correlation function.

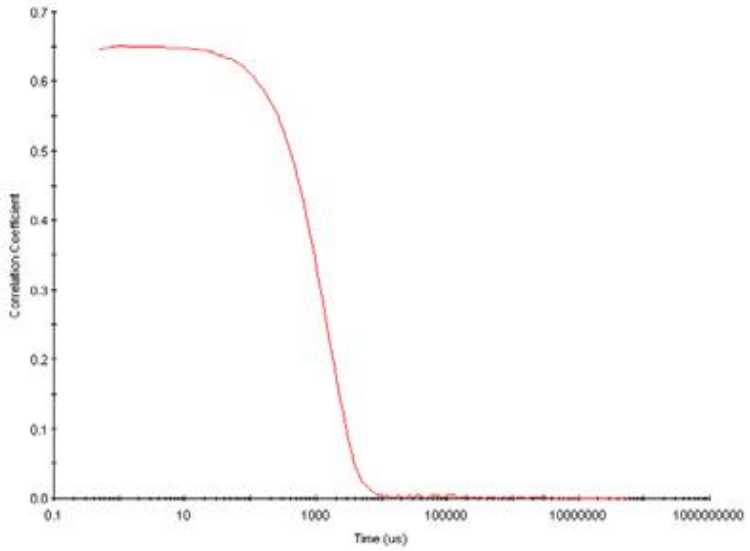

Figure 2.1a – Simulated correlation function for large particles[2]

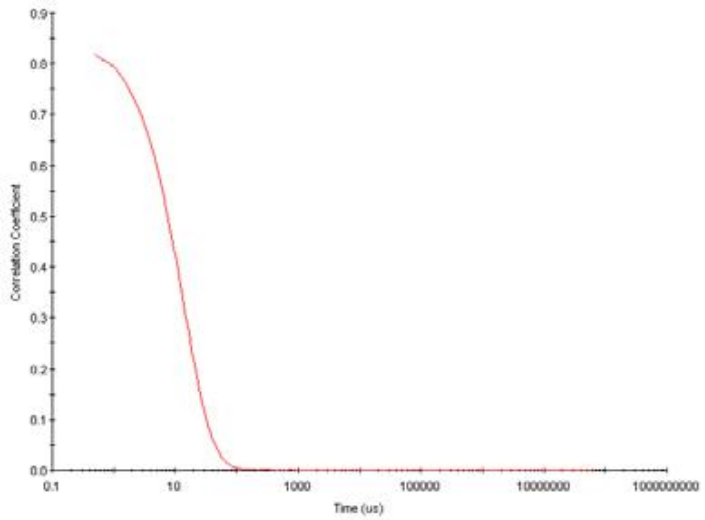

Figure 2.1b – Simulated correlation function for small particles[2]

Since PCS depends upon measuring the intensity of light scattered by Brownian motion of particles, several parameters are important to ensure an accurate measure of the particle size. A stable measurement temperature is essential to reduce non-random motion produced by convection currents and to obtain a valid viscosity value for the suspension fluid, since particle velocity cannot otherwise be calculated. The velocity of the Brownian motion is defined by a property called the translational diffusion co-efficient (D) and the size of the particle calculated from this value by using the Stokes-Einstein equation;

$$D = \frac{k_B T}{6\pi\eta r} \qquad (2.2)$$

where k_B is the Boltzmann constant, T is the Kelvin temperature, η is solution viscosity and r is the particle radius.

This measured diameter is concerned with how a particle diffuses in a viscous medium, so is referred to as the hydrodynamic diameter and is the diameter of a sphere that has the equivalent translational diffusion co-efficient as the particle. This diffusion co-

efficient is dependent not only upon the size of the particle core but also upon the particle surface structure and the ionic strength in the solution. Changes to the surface of the particle, such as an extended polymer layer, will reduce the diffusion speed and result in a larger apparent size. The nature of the particle surface and polymer layers will also affect the polymer conformation and hence the apparent size. The ionic concentration of the solution will modify the thickness of the electrical double layer, Debye length (κ^{-1}), resulting in changes in diffusion speed. An extended double layer, due to low ionic strength can result in a high apparent size, whilst under high ionic strength the electrical double layer will be suppressed, leading to a reduction in the hydrodynamic diameter.

Since photon correlation spectroscopy is based upon the translational diffusion co-efficient of a sphere, it has difficulty describing the size of a non-spherical particle. However, if the particle being measured changes shape in a way that affects the diffusion speed then the changes will be detected i.e. for a rod shaped particle, changes in length will be detected whilst a change in width will not and similarly for coiled structures, conformation changes can be detected.

The correlator in a PCS instrument will construct the correlation function from the intensity of the scattered light taking into account the parameters discussed above. Size data is then obtained from this function by using various algorithms.

Two algorithmic approaches can be taken to analyse the correlation function, either fitting a single exponential or fitting a multiple exponential. Fitting a single exponential will obtain a mean size and a width of the distribution whilst fitting a multiple exponential will obtain the distribution of the particle sizes. This is known as an intensity size distribution[2]. If instead the intensity size distribution is recalculated on the basis of the scattering volume of the particles, the particle size distribution becomes weighted towards the most volume effective particle size distribution, hereafter referred to as a volume weighted particle size distribution. The most widely accepted method of determining the particle size distribution is the CONTIN method published by Provencher[3]. This is a non-linear least squares based approach to fitting inverse Laplace transformed correlation functions in order to determine the particle size distribution.

2.1.2 Theory

There are two main theories commonly used in PCS. These are, Rayleigh scattering for particles much smaller than the wavelength of light (approximately <λ/10) and Mie scattering for particles approaching the wavelength of light. When the particles are much smaller than the light wavelength, the scattering produced in the Rayleigh case is essentially isotropic, all the wavelengths are in phase and absorption can be considered as negligible. Rayleigh[4] showed that the intensity of the light is related to the size of the particles and wavelength of the light.

$$I = \frac{I_0 .16\pi^4 r^6}{d^2 \lambda_0^4}\left(\frac{\left(n^2-1\right)}{\left(n^2+2\right)}\right)^2 \quad (2.3)$$

where I = scattered intensity of light, I_0 = original intensity of light, d = distance of detector, r is the radius of the particle, λ_0 is the wavelength of incident light and n is the refractive index ratio of the particle relative to that of the continous phase, that is;

$$n = \frac{n_1}{n_o} \quad (2.4)$$

where n_o = refractive index of medium, n_1 = refractive index of particle

The scattered light intensity shows a sixth power dependence on the particle radius meaning that larger particles will scatter significantly more light than smaller ones and the signal for these particles will quite easily obscure that of the smaller particles. It is therefore difficult to measure a mixture of small and large particles using PCS. The inverse dependence on the wavelength of light used, λ_0^4, means that higher scattering intensity is also obtained when the wavelength of light is reduced.

As the particles approach the wavelength of the illuminating light, the behaviour of the scattered light is changed and a complex function of maxima and minima is seen with the detecting angle. The path length through the particle is now comparable to the

wavelength and absorption of light by the particle cannot be ignored. The propagation of an electromagnetic wave through a particle which scatters and adsorbs was solved by Mie[5] and is the only theory that fully explains the maxima and minima seen in a plot of intensity with angle. A full explanation of Mie theory is beyond the scope of this thesis.

2.1.3 Application

The correlation function for the intensity of the scattered light is translated into size data by fitting a multiple exponential (in Port Sunlight via the application of the CONTIN program) to obtain the distribution of the particle sizes. This is known as an intensity size distribution and is based largely on Rayleigh theory but can be weighted to the size of the particles if they are close to the Rayleigh Gans Debye limit, where the particle diameter becomes a significant fraction of the wavelength of the light and the scattered light from different parts of the particle has different distances to travel to the detector. This intensity distribution can be converted to either a volume or number distribution using Mie theory which can give a more realistic view of the size variation of particles present in the sample. If there is a mixture of particle sizes, the relative scattering intensities, as discussed earlier, will cause the large particles to drown out the smaller ones. A number distribution shows the number of particles in each size class, whilst a volume distribution coverts this to volume so 1:1 would become 1:1000 (based on $4/3\pi r^3$) where r is the particle radius. Thus, comparing the three distributions can give a true measure of the particles present in the system.

2.2 Electrophoretic Mobility and Zeta Potential

2.2.1 Principles

The Zeta potential is a physical property exhibited by particles in suspension. It is a useful parameter for the colloidal scientist since it can be used as an indicator of colloidal stability which can allow the likelihood of flocculation in a system to be determined and hence probable formulation stability.

Most colloidal aqueous suspensions carry an electric charge that originates from the nature of the particle and the surrounding medium. Commonly this is due to ionisation of surface groups, differential loss of ions or adsorption of charged species. This net charge at the surface affects the distribution of ions in the surrounding media, resulting in an increased concentration of counter ions close to the surface producing an electrical double layer around the particle. This inner liquid layer is known as the Stern layer and the ions are strongly bound. There is also an outer diffuse layer where the ions are less firmly bound and within this region a boundary within which the ions and particle form a stable entity. Ions within the boundary layer move with the particle whilst ones outside stay with the bulk solution. The electromotive force measured at this hydrodynamic shear surface is known as the zeta potential[6]. Figure 2.2 illustrates the nature of the electrostatics associated with a charged particle. If the zeta potential value is largely negative or positive then the particles will tend to repel each other and no flocculation will occur.

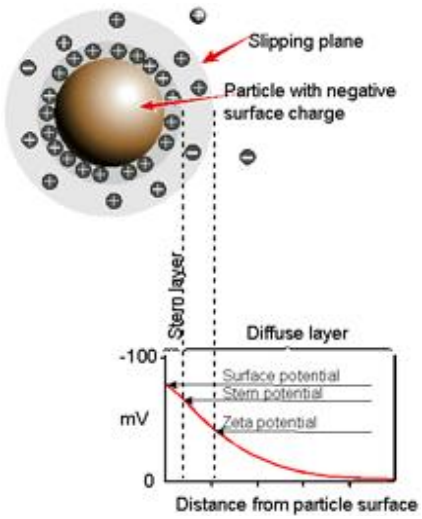

Figure 2.2 – Illustration of Electrostatic Layers Associated with a Charged Particle[6]

Due to the presence of surface charge on particles, they are able to interact with an applied electric field and, in the case of electrophoresis, this results in movement of the charged particles relative to the suspending medium. The charged particles are attracted

to the electrode of opposite charge whilst viscous forces of the medium tend to oppose this movement. When equilibrium is reached between the two forces then the particles move with a constant velocity. This velocity is dependent upon the strength of the electric field, the dielectric constant and viscosity of the medium and the zeta potential of the particles and this is usually termed electrophoretic mobility.

Essentially, electrophoresis is measured using a capillary cell with electrodes at either end to which an electric potential is applied. Particle velocity is measured as they move towards the electrode either manually, using microscopic techniques, or instrumentally via laser Doppler electrophoresis. This uses a laser light to illuminate the particles within the sample and the frequency shift of the light scattered by the particles is detected. If the particles are stationary, this scattered light has the same frequency as the incident light. However, when an electric field is applied, any moving particles will cause the scattered light to shift frequency proportional to the particle speed[7]. This shift in frequency is determined by combining the scattered and reference beams to obtain a modulated beam due to constructive and destructive effects with a much smaller beat frequency. This beat frequency is compared with that of a reference frequency and the size of the Doppler shift determined[8].

$$\Delta f = \frac{2\nu \sin\left(\frac{\theta}{2}\right)}{\lambda} \qquad (2.5)$$

where ν is the particle velocity, λ is the laser light wavelength, θ is the scattering angle and Δf is the frequency shift.

To enable measurement of low mobility or high conductivity samples, phase analysis light scattering is used to process the signal. Instead of measuring the frequency shift, this determines the phase shift as the measured phase change is proportional to the change in position of the particles. Measuring the phase difference between the beat and reference frequency allows changes in the particle position to be more accurately determined[9].

2.2.2 Theory

The velocity of a particle in a unit electric field is referred to as its electrophoretic mobility and is related to the particle velocity and hence the zeta potential using the Henry equation.

$$U_E = \frac{2\varepsilon\zeta f(\kappa a)}{3\eta} \qquad (2.6)$$

where U_E is electrophoretic mobility, ζ is zeta potential, $f(\kappa a)$ is Henry's function, ε is the dielectric constant and η is the viscosity of the medium.

The units of κ, the Debye length, are reciprocal Angstoms and κ^{-1} is often taken as a measure of the thickness of the electrical double layer. The parameter, a, refers to the radius of the particle and hence κa measures the ratio of the particle radius to the electrical double layer thickness.
The Debye length[10] can be illustrated by equation 2.7,

$$\kappa^{-1} = \sqrt{\frac{\varepsilon_r \varepsilon_0 k_B T}{2 N_A e^2 I}} \qquad (2.7)$$

where I is the ionic strength of the electrolyte, ε_r is the dielectric constant, ε_0 is the permittivity of free space, k_B is the Boltzmann constant, T is the temperature, N_A is the Avogadro number and e is the elementary charge.

If the diffuse layer is small compared to the particle radius then the diffuse layer can be treated as planar relative to the particle surface and the Smoluchowski equation can be used for electrophoretic mobility.

$$U_E = \frac{\varepsilon\zeta}{\eta} \qquad (2.8)$$

where U_E is electrophoretic mobility, ζ is zeta potential, ε is the dielectric constant and η is the viscosity of the medium.

If the diffuse layer is large compared to the particle then the particle acts as a point charge and the diffuse layer slows the particle motion. This is due to the electrical force on the ions of the diffuse layer, as they try to migrate in the opposite direction to the particle due to their charge being the opposite sign. Thus we end up with the Hückel equation which gives lower mobility than that expected from the Smoluchowski equation[11].

$$U_E = \frac{2\varepsilon\zeta}{3\eta} \qquad (2.9)$$

where U_E is electrophoretic mobility, ζ is zeta potential, ε is the dielectric constant and η is the viscosity of the medium.

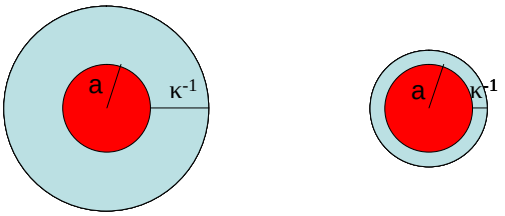

Hűckel Approximation
f(κa) = 1.0

Smoluchowski Approximation
f(κa) = 1.5

Figure 2.3 – Schematic Diagram Illustrating Changes in the Particle Diffuse Layer Related to the Hückel and Smoluchowski Approximations where κ is the Debye length and a is the particle radius[7]

The Henry equation allows for a smooth transition from the Hückel result to the Smoluchowski result with changes in the value of κa.

2.2.3 Application

Derjaguin, Verwey, Landau and Overbeek developed a theory in the late 1940s which investigated the stability of colloidal systems[12]. DVLO theory states that the stability of a particle in solution is dependent upon its total potential energy, which is the balance of competing forces.

$$V_T = V_A + V_R \qquad (2.10)$$

V_A is the contribution due to attractive forces known as the van der Waals attraction and can be expressed as follows:

$$V_A = \frac{-A}{\left(12\pi D^2\right)} \qquad (2.11)$$

where A is the Hamaker constant and D is the particle separation.

V_R is the contribution due to repulsive forces known as the electrical double layer repulsion and can be expressed as:

$$V_R = 2\pi\varepsilon a\zeta^2 \exp\left(-\kappa D\right) \qquad (2.12)$$

where a is the particle radius, π is the solvent permeability, κ is a function of the ionic composition, D is the particle separation and ζ is the zeta potential.

V_A and V_R are relatively large forces or potentials which act over a large distance and as particles approach each other due to Brownian motion, DVLO theory suggests that the sum of these forces between the particles will determine the stability of the dispersion. There is an energy barrier due to the repulsive force that prevents two particles approaching one another but if they collide with sufficient energy to overcome this barrier then the attractive force will pull them into contact and they will strongly and irreversibly adhere together. However, if the repulsive force is reduced, for example in high electrolyte conditions, then a secondary minimum can be produced where a weak, reversible adhesion between particles exists. In this case, the particles can be broken up again by applying shear. Figure 2.4 illustrates the variation in free energy with particle separation predicted by DVLO theory whilst Figure 2.5 illustrates the variation of free energy with particle separation in stabilised systems resulting in a secondary minimum.

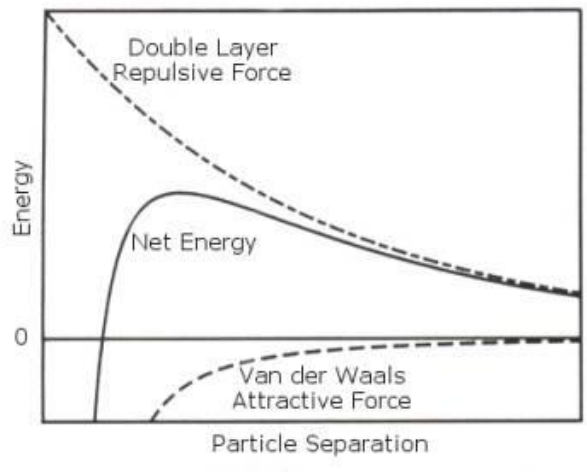

Figure 2.4 – Illustration of the Variation in Free Energy with Particle Separation predicted by DVLO theory[7]

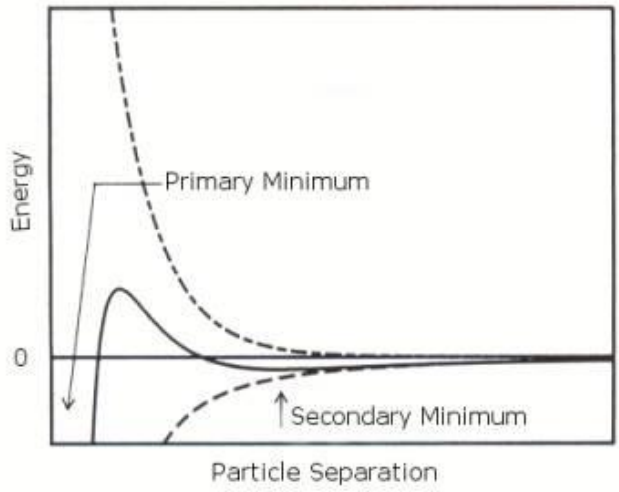

Figure 2.5 – Illustration of the Variation of Free Energy with Particle Separation in Stabilised Systems[7]

To maintain the stability of a colloidal system, the repulsive forces must dominate and this can be achieved via two mechanisms. Steric repulsion involves adding polymers into the system which adsorb onto the particle surface. If the polymer coating is sufficiently thick, the particles are separated due to steric repulsions between the polymer layers and hence do not come into contact and cannot adhere together. The amount and state of the polymer in the system is important otherwise hetero-flocculation can occur due to bridging or charge-patch formation. Electrostatic or charge stabilisation is where the species in the system are charged hence the double layer repulsive force is high and the particles are kept separate. The Zeta potential is a good indicator of the strength of the electrical double layer and hence the stability of a charge stabilised system.

2.3 Quartz Crystal Microbalance with Dissipation (QCM-D)

2.3.1 Principles

QCM has been used for over 50 years to measure mass changes on rigid surfaces. Traditionally it was used in either air or a vacuum[13] but more recently it has been shown to be an effective measurement in the liquid phase[14]. A QCM consists of a thin quartz disc sandwiched between a pair of electrodes. Due to the piezoelectric properties of quartz, an AC voltage applied across the electrodes can excite the crystal to oscillate at a specific frequency. This frequency can be related to changes in mass on the quartz surface, including water coupled to the oscillation. When a thin film is attached to the crystal, the resonance frequency decreases and this can be related to the mass of the film. If the film is rigid then the mass of the layer can be calculated using the Sauerbrey equation[13] in liquid,

$$\Delta f = \Delta m f_0^{3/2} \left(\frac{\eta_l \rho_l}{\pi \rho_q \mu_q} \right)^{1/2} \qquad (2.13)$$

where Δf is the measured frequency shift, f_0 is the resonance frequency of the fundamental mode of the crystal, η_l is the viscosity of the liquid in contact with the crystal, ρ_l is the density of liquid in contact with the crystal, ρ_q is the density of quartz ($2.648 g/cm^3$) and μ_q is the shear modulus of quartz (2.947×10^{11} g/cms^2).
This can be simplified to:

$$\Delta m = \frac{-C.\Delta f}{n} \qquad (2.14)$$

where Δm is the mass of the layer, C is 17.7ng Hz^{-1} cm^{-2} for a 5MHz quartz crystal and n is 1,3,5,7 etc. the overtone number.

It is also possible to calculate the volume of the adhering layer,

$$d_{eff} = \frac{\Delta m}{\rho_{eff}} \qquad (2.15)$$

where ρ_{eff} is the effective density of the adhering layer.

However, often the film is not rigid and hence will not fully couple to the oscillation of the crystal leading the Sauerbrey equation to underestimate the mass at the surface. QCM-D therefore measures both frequency and dissipation of the crystal. Dissipation occurs when the driving voltage to the system is shut off and the energy from the oscillating crystal dissipates from the system.

Dissipation is defined as,

$$D = \frac{E_{lost}}{2\pi E_{stored}} \qquad (2.16)$$

where E_{lost} is the energy lost during one oscillation cycle and E_{stored} is the total energy stored in the oscillator.

When molecules adsorb to the crystal surface, water (or other liquid), couples to the adsorbed material as an additional dynamic mass via hydration or entrapment within the adsorbed film. By measuring the dissipation, it can be determined if the film is rigid or viscoelastic. The amount of water can be high depending upon the type of material and surface. Elongated molecules could adsorb flat at the surface, hence little water is coupled to the film and a low dissipation value obtained. However, if they adsorbed perpendicular to the surface, the adsorbed water content would be high and the film highly dissipative. The frequency and dissipation data from both the fundamental frequency and multiple overtones are measured and this is illustrated in Figure 2.7. This enables simulations to be applied using a Kelvin-Voigt based viscoelastic model to obtain quantitative analysis of the adsorbed viscoelastic films[15].

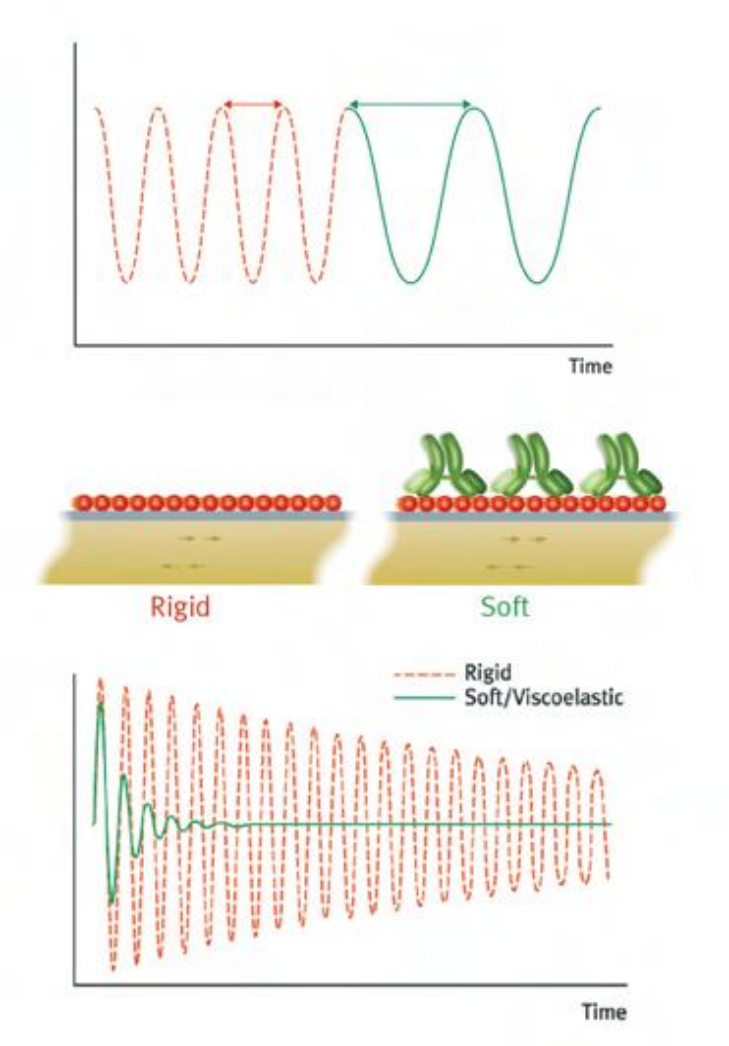

Figure 2.6 – Crystal oscillation under applied voltage (top graph) and dissipation of crystal oscillation with voltage removed (bottom graph). Signals for hard materials (red) and soft materials (green) absorbed onto a crystal[15]

2.3.2 Theory

The changes in frequency and dissipation can be modelled using a Kelvin-Voigt model. The system is modelled as a thin film attached to the quartz crystal and covered by a semi-infinite Newtonian bulk fluid where the bulk fluid is described by its density (ρ_o) and viscosity (η_o), and the thin film by its density (ρ_f), shear modulus (μ_f), shear viscosity (η_f) and thickness (δ_f). It is assumed that the film covers the sensors entire area, is homogeneous and has uniform thickness. It is treated as a Kelvin-Voigt element, defined as a spring and dashpot in parallel under no slip conditions[16]. Data is interpreted

with an elastic model where η_f is held at zero, then by a viscous model where μ_f is held at zero and finally by a visco-elastic model where all parameters are varied and the best fit to the measured data obtained. This then enables storage and loss modulus of the system to be calculated by,

$$G^* = G' + iG'' = \mu_f + i2\pi f\eta_f \qquad (2.17)$$

using μ_f and η_f previously calculated by the model (where *f* refers to the thin attached film) and allowing interpretation of the film behaviour.

2.3.3 Application

QCM-D has been used extensively to enable real time measurements of both mass and structural properties of molecular layers. Measuring both frequency and dissipation over several harmonics allows viscoelastic models to be tested[16]. These can give accurate analysis of soft films that do not follow the standard linear relationship between change in crystal frequency and change in adsorbed mass. The technique also allows the researcher to follow the kinetics of adsorption of various systems onto surfaces and the solution properties can easily be changed.

2.4 Dynamic Secondary Ion Mass Spectroscopy

2.4.1 Principles

Dynamic SIMS can provide quantitative information on the elemental composition of a sample surface region from a few nm to several microns in depth with the detection sensitivity in the ppm to ppb range for all elements in the periodic table. A primary ion gun produces a beam, with the energy range 0.5 keV to 20 keV, and this primary beam can be O_2^+, O^-, Cs^+ or Ar^+. Commonly, O_2^+ is used for the detection of electropositive species and Cs^+ for electronegative species. When the primary beam hits the sample, it leads to the ejection of surface atoms, a fraction of which are ionised and known as secondary ions. These are accelerated into a secondary column where they can be

filtered according to their direction of travel, mass or energy then finally concentrated on the detector. A mass spectrum of the sample surface can be produced or, if several elemental species are studied with time in the same sample area, a depth profile for that ion can be obtained.

2.4.2 Theory

As the primary ion beam bombards the sample, the sample material is able to slow down and stop an incident ion[17]. For the energy range used in SIMS, this is due to the nuclei stopping power which is related to direct collisions between the primary ion and the target atoms nuclei. Sputtering is the result of the ion momentum transfer towards the target atoms and is dependent upon the energy transferred by the incident ion. For low energy ions (<100eV) the energy transferred may eject atoms but is too weak to cause a collision series involving two or more atoms (<1000eV). If the energy is higher than 1000eV all the atoms near the incident ion impact site are moved and local warming also results. As all local atoms are affected, a disturbed zone occurs which limits the ability to measure depth profiles. The impact energy, E_{impact}, is also affected by the secondary acceleration voltage, which speeds up the secondary ions, by the equation,

$$E_{impact} = \frac{q}{e}.(U_1 - U_2) \qquad (2.18)$$

where E_{impact} is measured in eV, U_1 is the primary ions acceleration voltage, U_2 is the secondary ions acceleration voltage, q is the electric charge of one primary ion and e is the elemental electric charge.

If the primary ions are Cs^+ or O_2^+ then the relationship can be simplified to,

$$E_{impact} = (U_1 - U_2) \qquad (2.19)$$

So for positive secondary ions, the sum of the two voltages produces a reduced impact energy and hence good depth resolution. The incident angle of the primary beam also

affects the impact energy and again positive secondary ions are shown to be favourable for depth resolution.

The sputtering yield is defined as the average number of atoms ejected by one ion impact and depends upon the primary ions energy, mass and incidence angle plus the nature of the sputtered material. If we assume the material is amorphous and the primary ions are low energy then the sputtering yield, η_{pulve}, is proportional to the ratio,

$$\eta_{pulve} \propto \frac{E_{impact}}{U_s} \qquad (2.20)$$

where E_{impact} is the impact energy of primary ions and U_s is the binding energy of surface atoms.

Of these sputtered atoms and molecules, only a small fraction are ionised to produce the secondary ions for detection. For a species, i, the ionisation rate is as follows,

$$\alpha(i) = \frac{N_{ion}(i)}{N_0(i)} \qquad (2.21)$$

where N_{ion} (i) is the number of ionised particles and N_o (i) is the total number of sputtered particles.

This rate is dependent upon the electronic properties of the species itself and the properties of the atoms surrounding it in the sample. Therefore the nature of the primary ions is important as these are heavily implanted into the sample layers. Generally, the particles sputtered by the primary ion bombardment are monoatomic unless the element tends to remain neutral, in which case polyatomic ions are detected.

2.4.3 Application

Due to the parameters discussed above, three main analysis types are realistic in DSIMS. These are,

1. O_2^+ primary ions and detection of positive secondary ions.
2. Cs^+ primary ions and detection of negative secondary ions.
3. Cs^+ primary ions and detection of polyatomic positive ions.

DSIMS can measure major and minor elements present in a material by local sputtering of a sample and collection and analysis of the secondary ions produced. These are analysed by a mass spectrometer and can result in identification of the elements present on the surface or even a 2-dimensional map. The presence of the element as a function of depth in the sample can also be determined and if a standard is used then concentration profiles may also be obtained.

2.5 Conductivity

Electrical conductivity is the ability of a substance to carry electrical current. In water, this electrical current is carried by ions since electrons do not pass through water themselves, thus, it can be used as a measure of the purity of water or the level of ionic species present. A voltage is applied between two inert electrodes immersed in a solution, resulting in the ions between them being attracted to the electrode with opposite charge. Ions will therefore move between electrodes and produce a current that is dependent on the electrical resistance of the solution.

However, conductivity measurements are non-specific and cannot distinguish between different types of ions, only give a reading proportional to all the ions present. Some ions will contribute more than others[18]. Conductivity is the conductance of a volume of water with a $1cm^2$ cross-sectional area and electrodes spaced 1cm apart. This has a cell constant of $1cm^{-1}$ but other cell constants can be used as long as the measuring instrument readout is normalised allowing for measurement of more dilute solutions. The cell constant is a function of the electrode areas, the distance between the electrodes and the electrical field pattern between the electrodes. This type of measurement is

known as an amperometric system where a known potential is applied to the electrodes and the current measured. Polarisation may cause a depletion of anions or cations around the electrode due to charge build-up and will lead to lower readings than expected. This can be reduced by using high frequency AC in measurements and controlling the current density. For greater accuracy and at higher conductivity levels, a potentiometric method is used, which is based on induction and uses 4 rings. The two outer rings apply an AC voltage and induce a current loop in the solution while the two inner rings measure the voltage drop due to the current loop[19]. Conductivity is also affected by temperature due to the nature of the ions and the fact that water becomes less viscous. Most ions increase conductivity at a rate of 2.2% per °C but at low ionic concentrations the ionisation of the water becomes a more significant part of the conductivity and this changes to ~5% per °C. At high ionic concentrations, ionic interference restricts the movement of ions and the conductivity can reach a plateau. The temperature influence also decreases to about 1.5% per °C. Conductivity is generally expressed in Siemens or for dilute solutions micro- or milli-Siemens.

2.6 Streaming Potential

Streaming potential is a measure of the electric field generated when a liquid is forced to flow past a stationary charged surface. A pressure gradient is applied which sets the liquid in a capillary tube in motion. The double-layer charge moves with the surrounding liquid giving rise to an electric current. After a short time, due to charge transfer, the current due to the pressure gradient is balanced by the current due to the induced electric field and this leads to a drop in potential known as the streaming potential U_s [20]. It can be related to zeta potential as follows:

$$U_s = \frac{\zeta \varepsilon \varepsilon_0 \Delta_p}{\eta K_e} \qquad (2.22)$$

where ζ is the zeta potential, ε is the relative dielectric constant, ε_0 is the absolute dielectric constant, Δ_p is the pressure difference, η is the viscosity and K_e is the electrical conductance.

Streaming potentials can be measured at flat surfaces[21] or packed beds or fibres or particles. In order to minimise the polarisation of the electrodes, measurements should be performed with the liquid flowing in both directions. Care should also be taken to avoid turbulence due to high flow rates or changes in the flow through a packed bed.

2.7 Scanning Electron Microscopy

Scanning electron microscopy (SEM) uses electrons instead of light to form an image and has many advantages over a traditional light microscope. It has a much higher resolution and larger depth of field which allows a higher level of magnification and a larger focus area. SEM also uses electromagnets instead of lenses to focus the beam, thus giving more control over the magnification[22].

An electron beam is generated from a source commonly consisting of a tungsten gun. A voltage is applied to a loop of tungsten which acts as the cathode. The anode then attracts electrons from the heated filament and causes them to accelerate, some bypassing the anode and passing on down the column. This beam then travels through various electromagnetic fields and lenses to focus the beam as a fine point onto the sample. Once the beam hits the sample, electrons and x-rays are emitted, which are collected by detectors, converted to a signal and sent to a cathode ray tube which produces the final image. Commonly, the primary backscattered electrons, secondary electrons and X-rays are used to extract information about the sample.

Since an electron beam is used, SEM is performed under vacuum conditions. Otherwise high instabilities will occur in the beam. Samples must therefore be carefully prepared as all water must be removed to avoid vaporisation under vacuum and the sample must be conductive. Metals need no extra preparation but non-metals are covered with a thin layer of conductive material using a sputter coater. The sample is placed under vacuum and an electric field is used to produce argon ions from argon gas. These are attracted to a negatively charged gold foil, knock gold atoms from the surface and these fall on the sample to produce a thin gold coating.

2.8 References

1. Berne B.J.; Pecora R., Dynamic Light Scattering; Wiley: New York, 1976
2. Malvern DLS Technical Notes MRK656-01
3. Provencher, S.W., Makromol Chem **180** (1979) 201
4. Born M., Wolf E., Principles of Optics 5th Ed, Pergamon Press, Oxford, (1975)
5. Mie G., Ann Phys, Leipzig, 25 (1908), 377-445
6. Goodwin J.W., Colloids and Interfaces with Surfactants and Polymers, Wiley, Sussex (2004)
7. Malvern DLS Technical Notes MRK654-01
8. Malvern DLS Technical Notes MRK570-01
9. Malvern DLS Technical Notes MRK571-01
10. Russel W.B., Saville D.A., and Schowalter W.R., Colloidal Dispersions, Cambridge University Press (1989)
11. Hunter R.J., Zeta Potential in Colloid Science: Principles and Applications, Academic Press, UK (1988)
12. Goodwin J.W., Colloids and Interfaces with Surfactants and Polymers, Wiley, Sussex (2004)
13. Sauerbrey G., Z Phys **155** (1959) 206-222
14. Konash P.L., Bastraans G.J , Anal Chem **52** (1980) 1929
15. Q-Sense QCM-D Technology Notes
16. Voinova M.V., Rodahl M., Johnson M., Kasemo B., Phys. Scr. **59** (1999) 391-396
17. Probion Analysis, Magnetic Sector Secondary Ions Mass Spectrometry Analysis Information Literature
18. Aquarius Technical Bulletin 008, Version 2 (August 2000)
19. Elements of Physical Chemistry, Macmillan (1903)
20. Hunter R. J., Foundations of Colloid Science – Volume 1, Clarendon Press, Oxford (1995)
21. Fa K.Q., Paruchuri V.K., Brown S.C., Phys. Chem. Chem. Phys **7** (2005) 678-684
22. Amelinckx S., van Dyck D., van Landuyt J., van Tendeloo G., Electron Microscopy: Principles and Fundamentals, Wiley (2007)

3 Experimental Practical

3.1 Materials

The non-modified and modified silica samples were obtained from Grace Davison, USA. Ludox HS is an unmodified colloidal silica dispersion with a specific surface area of 198-258m^2/g, which is about 12 nm average particle size. Figure 3.1 shows the surface configuration of a Ludox HS particle as defined by the supplier (the particle is spherical but drawn exaggerated for detail). The surface is covered with silanol groups and stabilised by negative charges from partial ionisation with sodium counter-ions associated with the surface.

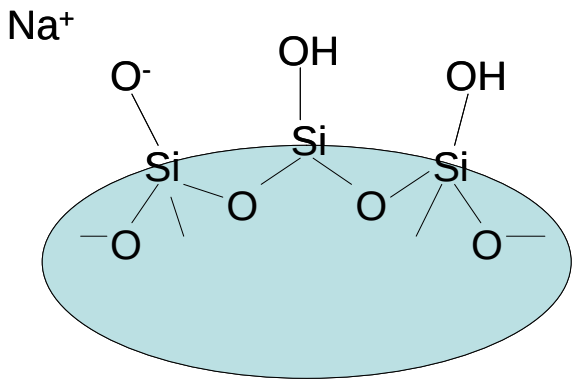

Figure 3.1 – Schematic of the Surface Configuration of Ludox HS Unmodified Silica

Ludox CL is a modified colloidal silica dispersion where the Ludox HS particles are coated with aluminium oxide to reverse the surface charge from negative to positive. The modification involves using aluminium chloride and leaves about 3% aluminium oxide behind after the reaction. The particles have a specific surface area of 230m^2/g and are slightly larger than the Ludox HS particle due to the coating on the surface. Figure 3.2 shows the surface configuration of a modified Ludox CL particle as defined by the supplier (the particle is spherical but drawn exaggerated for detail).

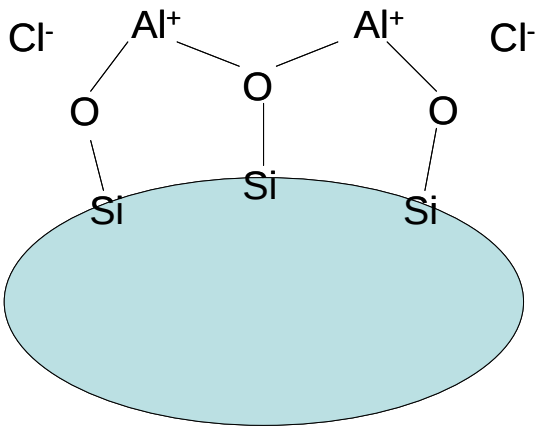

Figure 3.2 - Schematic of the Surface Configuration of Ludox CL Modified Silica

The Ludox CL surface is covered with aluminium oxide as Al_2O_3 and connected to the silica particle via the silanol oxygen associated with the silicon atom. The supplier literature does not state the layer thickness but it is likely to be of the order of several layers of Al_2O_3. Measurements in Chapter 4 give values of approximately 4nm.
Sodium chloride, aluminium chloride, HCl and NaOH were obtained from Sigma-Aldrich and used without further purification. Millipore water was used throughout.

3.2 Sample Preparation and Techniques

3.2.1 Photon Correlation Spectroscopy and Zeta Potential Measurements

Ludox HS is a 30% active dispersion in alkaline media with a natural pH of about 10. Ludox CL is a 30% active dispersion in acid media with a natural pH of approximately 3. For the PCS and zeta potential measurements and titrations, 1% dispersions were prepared in Millipore water by directly diluting the stock materials. For the titrations with electrolyte, again 1% dispersions were prepared by diluting the stock materials in Millipore water but the relevant amount of sodium chloride was first dispersed in the water.

PCS measurements were performed using a Malvern Zetasizer NanoZS fitted with a 50mW microgreen laser (JDS Uniphase) and 10nm bandpass filters at 532nm to minimise fluorescence. Measurements were taken at 173º backscatter mode using disposable Malvern DTS0012 cuvettes at 25ºC. Autocorrelation data was collected using 12 sub-runs of 10 seconds in triplicate then the CONTIN analysis model used to perform the result transformation[1]. Refractive index values for the materials were:

Ludox HS: 1.46 silica
Ludox CL: 1.713 coated sphere

Zeta potential measurements were taken on the same machine using a disposable DTS1060C zeta cell. 75-100 runs were taken per measurement with 40 measurements at 25V. Automatic data processing was used with automatic attenuator selection and the same RI parameters as above.

3.2.2 Quartz Crystal Microbalance with Dissipation Measurements

Measurements of the materials on the QCM were performed at $1x10^{-2}$% w/w, $1x10^{-3}$% w/w and $1x10^{-4}$% w/w dispersion concentrations. All concentrations were made by diluting the stock materials with Millipore water. To ensure the required pH values, the Millipore water was first adjusted to either pH 3, 5 or 10 using sodium hydroxide or hydrogen chloride.
Measurements were performed on a Q Sense E4 QCM-D which allowed simultaneous measurements of four AT-cut quartz crystals with a silica surface. Each crystal was washed in ethanol and UV-ozone cleaned to remove contaminants, then dried under filtered nitrogen gas before being placed in the chamber[2]. Initially, all crystals were exposed to water to obtain a baseline for the frequency and energy dissipation. Ludox dispersions were then introduced into the measurement chambers at a rate of 300µl/min until the water was displaced and measurements taken until deposition had ceased. In all cases, a water rinse was then performed to see if detachment occurred. A schematic of the setup can be seen in Figure 3.3.

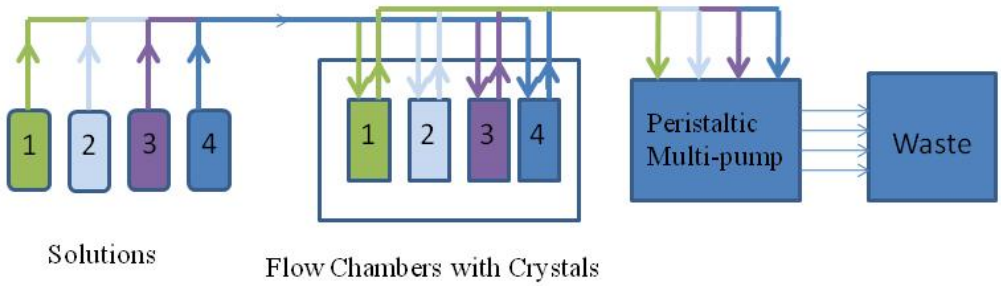

Figure 3.3 – Representative schematic experimental set-up for the Q Sense E4 QCM-D

3.2.3 Other Techniques

3.2.3.1 Scanning Electron Microscopy

QCM crystals were allowed to dry on removal from the machine. Then each quartz disc was mounted onto an SEM stub using an adhesive carbon tab. One edge of each disc was tagged with a silver paint. They were subsequently coated with ~4 nm of Pt/Pd metal using a Cressington 208HR sputter coater and examined in a Hitachi S4700 SEM at magnifications between 15x and 150x.

3.2.3.2 Conductivity

Measurements were performed on a Jenway 4310 meter using a glass bodied conductivity/ATC probe. Calibration curves were prepared with both sodium chloride and aluminium chloride at $1x10^{-5}$ M to $1x10^{-3}$ M solution concentrations in Millipore water and measurements obtained in microSiemens. The diluent obtained from the Ludox CL dialysis experiment was measured and compared to the calibration curves to estimate the amount of aluminium leached from the surface of the particles.

3.2.3.3 Streaming Potential

Streaming potential measurements were performed on Anton Paar Electro Kinetic Analyser (EKA). A rectangular cell was used in which laminar flow is established

between two parallel plates. In this case, silica wafers were placed in the cell and a 1mM KCl solution was allowed to flow through the measuring cell to obtain the streaming potential of the wafers. A $1x10^{-5}$M solution of aluminium chloride was allowed to flow through the cell to simulate the aluminium ions produced by the modified Ludox CL dispersion and the KCl solution repeated to observe any changes in the potential of the silica wafer. All silica wafers were rinsed in water and annealed before use. A schematic of the cell can be seen in Figure 3.4.

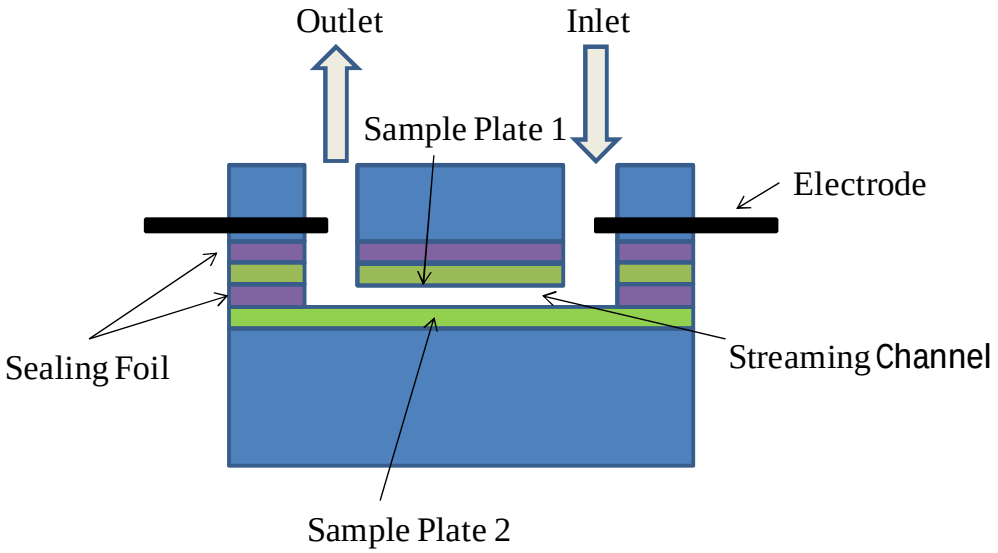

Figure 3.4 – Schematic of the rectangular streaming potential cell.

3.2.3.4 Dynamic Secondary Ion Mass Spectrometry

DSIMS can measure major and minor elements present in a material by local sputtering of a sample and collection and analysis of the secondary ions produced using a mass spectrometer. This can result in identification of the elements present on the surface.

DSIMS analysis was carried out using a Cameca ims 4f instrument. Since the deposited layer of aluminium was likely to be relatively thin, low energy ion bombardment conditions were utilised, under a 2.8keV $O2^{+}$ primary ion beam with ~30nA beam current. Profiles were acquired from an area of ~200µm x 200µm from the three samples. Crater depths were measured using a white light interferometer. Silica wafers were rinsed in water and annealed before use. The wafers were then soaked in either

Millipore water or a $1x10^{-5}$M aluminium chloride solution for 1 hour before being removed and allowed to dry naturally overnight.

3.3 References

1. Provencher S.W., Makromol Chem **180** (1979) 936
2. Webb, K. PhD Thesis Manchester University (2010) P.91

4 Results

4.1 Materials

Detailed information about the particles used has been given in the previous chapter. For convenience, a summary of the characteristics of each material is shown in Table 4.1.

Material	Specific Surface Area m^2/g	Particle Size nm	Particle Charge	Surface Groups
Ludox HS	258	12	Negative	Silica
Ludox CL	230	20	Positive	Alumina

Table 4.1 – Ludox material characteristics as defined by the supplier

In brief, Ludox HS is an unmodified colloidal silica dispersion received as a 30% active dispersion bearing weak negative surface charges. In contrast, Ludox CL, also obtained as a 30% active dispersion with the material containing chloride counter-ions associated with the alumina surface[1], is a type of modified colloidal silica coated with aluminium oxide to reverse the surface charge from negative to positive. The aluminium oxide is connected to the silica particle via the silanol oxygen associated with the silicon atom.

4.2 Surface Characterisation

A series of repeat measurements of electrophoretic mobility and particle size was performed on both Ludox HS (unmodified silica dispersion) and Ludox CL (modified silica dispersion) under their original solution conditions in water. Electrophoretic mobility was measured and converted to zeta potential using the Henry equation whilst particle size was measured using photon correlation spectroscopy.

Table 4.2 shows the intensity and volume averaged size for each dispersion derived from photon correlation spectroscopy. The intensity size distribution is dependent on

the scattered light intensity that has a sixth power dependence on the particle radius (according to Rayleigh). This means larger particles will overwhelm the signal from smaller particles due to the fact that they scatter significantly more light. If the intensity size distribution is recalculated on the basis of the scattering volume of the particles, a volume weighted particle size distribution is obtained that is weighted towards the most volume effective particle size distribution and is less affected by any polydispersity of the sample. This explains the differences seen in Table 4.2 where the volume weighted average is lower than that of the intensity weighted average. Ludox HS should be a monodispersed silica dispersion of the size 12 nm carrying negative charges. Monodispersity is the relationship between the intensity weighted distribution and the intensity number distribution defined as:

$$Monodispersity \approx \frac{\bar{z}(w)}{\bar{z}(N)} - 1 \qquad (4.1)$$

If this ratio is less than 0.2, a material is regarded as monodisperse. Data derived from particle size measurements in Table 4.2 show that the Ludox HS is in fact slightly larger than quoted in the literature and polydisperse. Ludox CL is also expected to be a monodispersed material about 20 nm in size carrying positive surface charges. This is because Ludox CL particles have been surface modified with a coating of aluminium oxide, resulting in the larger size due to the alumina layer formed on the silica surface. Again, the Ludox CL dispersion is slightly larger than stated but it is monodisperse. The differences in polydispersity can be attributed to the manner in which the particles grow. Silica particles are usually prepared by the hydrolysis of tetraethyl-orthosilicate with ammonia in alcohol[2], starting from silica nuclei formation. During the synthesis process, fresh nuclei are formed whilst existing nuclei are growing, resulting in polydispersity. The aluminium oxide coating is grown on top of the existing silica particles and since no fresh nuclei should form, the growth of the particles over time leads to a reduction in polydispersity[3]. In fact, the aluminium oxide coating grown onto the unmodified particle is of the order of 5 nm thickness, equivalent to that usually found growing on aluminium surfaces. The errors given below are due to the Gaussian width of the exponential associated with the measurement technique and bear no relationship to the

polydispersity. The zeta potential measurements show the expected values as stated in the literature for both products. The errors for the zeta potential are large due to the manner in which it is calculated from the phase difference between the beat and reference frequency. Smaller particles move more quickly and are therefore harder to detect, leading to increased difficulty in measuring the frequency shift and a larger error. The Ludox HS unmodified silica has a negative value whilst the Ludox CL modified silica has a positive value similar to alumina.

	Ludox HS	**Ludox CL**
Intensity Average nm	25 ± 9	40 ± 21
Volume Average nm	17 ± 7	27 ± 13
Polydispersity	0.363	0.164
Zeta Potential mV	-37 ±16	44 ± 12

Table 4.2 – Intensity and volume weighted particle sizes (diameter) of modified (Ludox CL) and unmodified (Ludox HS) silica particles

4.3 Ludox HS Unmodified Silica

The usual pH range of interest for personal products is between 4 and 7. The unmodified silica dispersion was characterised at the pH range of interest as previously using electrophoretic mobility and photon correlation spectroscopy. For ease, intensity averages are shown, as this is the software default mode. Although volume weighted averages would give a more accurate value for the actual particle size, they were difficult to extract from the software display. Both sets of values however give consistent trend of particle diameters.

4.3.1 Solution Chemistry

4.3.1.1 Zeta Potential in the pH Range 5-7

The variation in zeta potential with solute concentration over the pH range 5 to 7 is shown for Ludox HS with no added electrolyte in Figure 4.1. This is a colloidal silica dispersion in an alkaline medium and as such, at the natural pH 9-10, the surface is covered with ionised silanol groups. As the pH is reduced to the required pH range the number of ionised surface silanol groups will decrease but enough to remain dissociated to result in a negative surface charge, thus still rendering the dispersion kinetically stable.

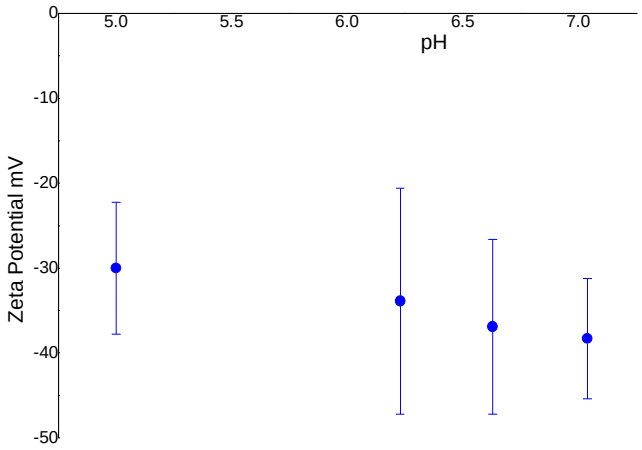

Figure 4.1 –Variation of Zeta potential values of unmodified silica dispersion Ludox HS in the pH range 5-7.

4.3.1.2 Particle Size Distribution in the pH Range 5-7

The intensity weighted particle size data over the pH range 5 to 7 for Ludox HS is shown in Figure 4.2. The particles have an average size of 20 nm across all pH values measured. Since the zeta potential shows that the silica surface charge is unchanged and the electrical double layer repulsive force is high, the size would be expected to remain

consistent as the particles are kept separate and the diffusion coefficient is not affected by the minor change in pH.

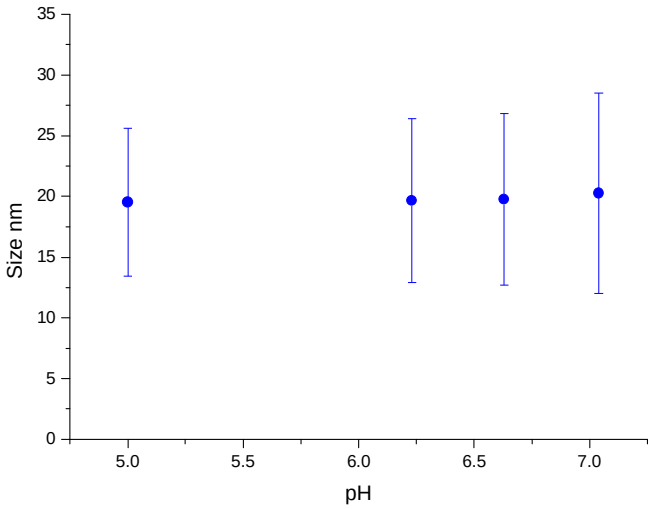

Figure 4.2 – Variation in intensity weighted particle size of Ludox HS umodified silica dispersion over the pH range 5-7

4.3.1.3 Particle Dispersion Behaviour in Other pH Ranges

As already indicated, the Ludox HS material is supplied as a dispersion in alkaline solution at pH 9-10. It is of interest to determine how changes in pH past the area of interest affect the stability of the colloidal particles hence a titration of Ludox HS against acid and alkali was performed to observe the dispersion characteristics. Figure 4.3 shows this pH titration for Ludox HS with no electrolyte. The titration was performed from the natural pH of about 10 to pH 3.8 and the effect on zeta potential and particle size distribution was observed.

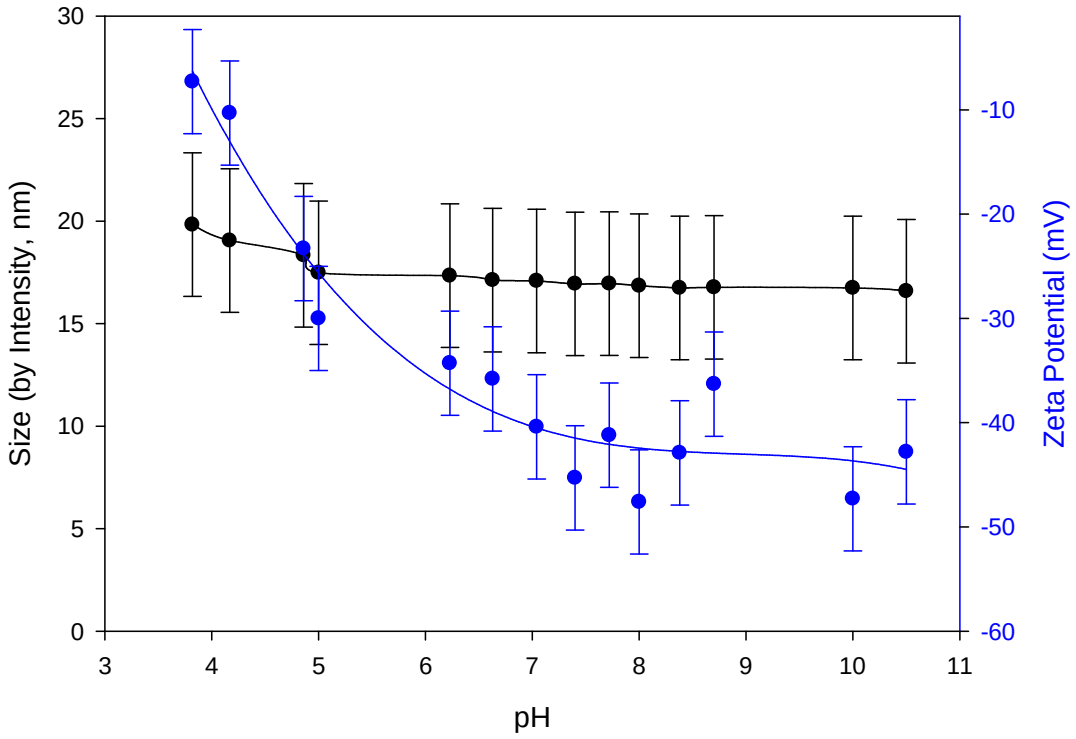

Figure 4.3 – Variation of the intensity weighted particle size and Zeta potential data for unmodified silica Ludox HS when titrated against acid from pH 10 to pH 4.

Since the surface charge will change due to the reduction of SiO- groups to Si-OH, the zeta potential will decrease from a high negative value to zero. There is now a reduced electrostatic barrier to overcome and changes occur in the electrical double layer hence producing changes in the diffusion coefficient. Since both electrophoretic mobility and PCS techniques are dependent upon the diffusion coefficient, any perceived changes are likely to be a consequence of these changes. In the pH titration above, the zeta potential is seen to decrease with pH and in turn, the average size of the particles starts to increase especially as the zeta potential tends towards zero but the material is still colloidally stable.

Figure 4.4 shows the alkali pH titration of Ludox HS from pH 4 to pH 10, performed immediately after the previous measurement. The surface potential of the particle recovers and the zeta potential becomes highly negative due to the increasing hydroxyl

ion content reacting with the surface silanol groups thus leading to ionisation. It should be noted that the variation in particle size is of the order of 9 nm and although the trend exists, the absolute value is probably within the experimental error of the machine.

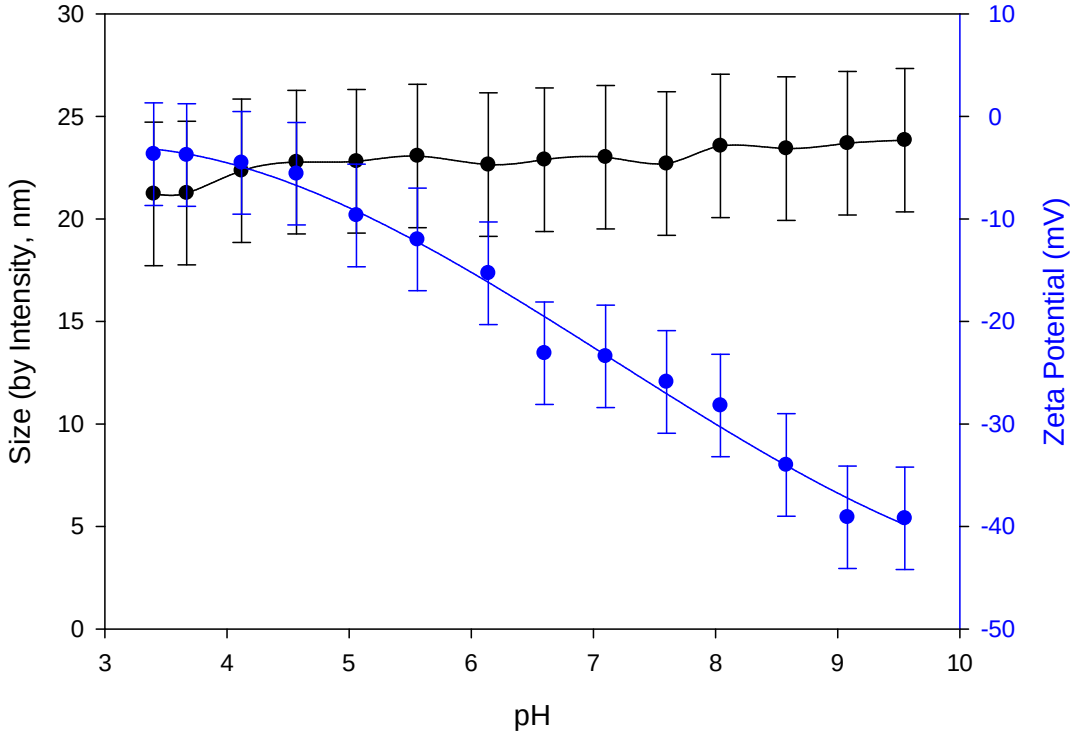

Figure 4.4 – Variation of the intensity weighted particle size and Zeta potential data for unmodified silica Ludox HS when titrated against alkali from pH 4 to pH 10.

4.3.2 Deposition onto Surfaces

4.3.2.1 Quartz Crystal Microbalance

Measurements were performed on two different machines. The KSV machine allows single measurements made on a static system. The material was introduced onto the QCM crystal and allowed to deposit with no flow. The rinse step involved introducing water alone and observing any removal that occurred. The Q-sense machine was capable of measuring four crystals at the same time. The material of interest flowed over the crystal at a fixed rate and measurements were taken of the amount of material

adsorbed. Hence, in the first case we had a quasi-diffusion system whilst in the second system we had a convection system as the solution was in constant flow so diffusion did not dominate. This could lead to differences in the deposited amount as in the convection system the material would be deposited and removed during the experiment.

In all cases, plain silica surfaces were used as the hydrophilic substrate. Silica, as discussed previously, carries a negative electrostatic charge in the pH range of interest. Figure 4.5 shows the streaming potential values of a plain silica slide[5].

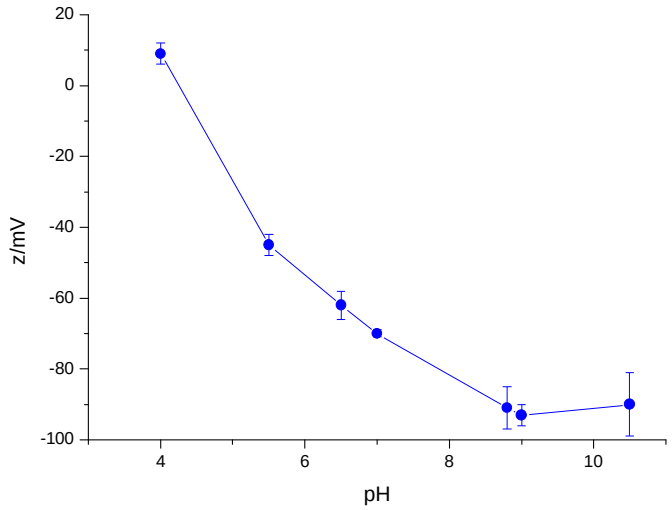

Figure 4.5 – Streaming Potential Values for a Plain Silica Wafer with Changes in pH.

Measurements were performed on the unmodified silica at three levels and at pH 10 (natural pH) and 5 (pH of interest). The concentrations of material for this experiment were limited by the sensitivity of the technique[6] as it was essential to remain in the linear response region.

Since the deposited material is silica in all cases, it can be treated as a rigid layer allowing for the Sauerbrey equation to be applied to all measurements obtained. This allows for changes in the resonance frequency to be directly related to the mass of the deposited film, see Chapter 2 equation 2.16 for details. Measurements are expressed as deposited amount in ng/cm^2 calculated from the 5th overtone. Figure 4.6 shows the

Ludox HS material deposited onto a silica crystal using the Q-sense machine and hence the convection system. In this case, due to the flow, particles are constantly brought into contact with the surface and also removed if they do not adhere strongly. In this case the material is at the natural pH of 10 and carries a large negative charge as most of the silanol groups are ionised. Since the silica crystal surface will also carry a large negative charge at this pH, deposition would not be expected to occur and Figure 4.6 illustrates that this is the situation. Variations seen in the data are random events and not meaningful since there is no consistent growth of material which would be expected if deposition was occurring. It is also probable that the high pH is affecting the silica crystals thus possibly contributing to some erroneous negative values and dissolution of the silica surface may occur.

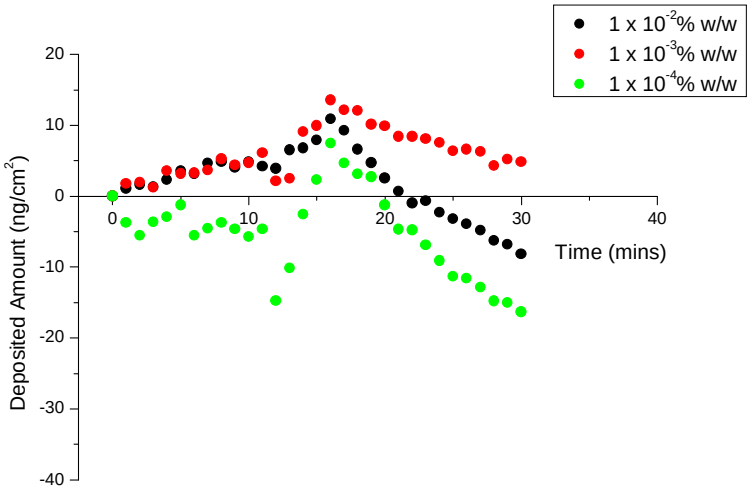

Figure 4.6 – The variation in mass versus time as a function of concentration for Ludox HS deposited onto a Silica QCM-D Crystal at pH 10 using the Q-Sense System.

Figure 4.7 shows the Ludox HS material deposited onto a silica crystal using the Q-sense machine at pH 5. Solution chemistry measurements have shown that the material still carries a large negative charge at this pH due to ionised silanol groups and since the silica crystal surface will carry a negative charge, deposition would not be expected to occur. This is clearly illustrated in Figure 4.7.

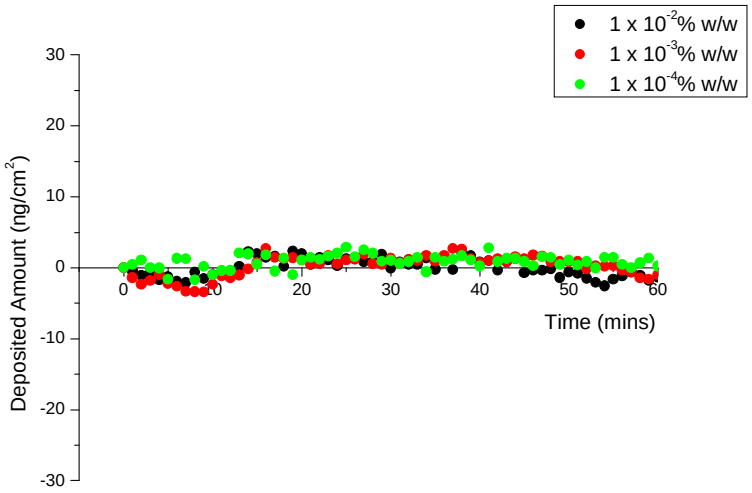

Figure 4.7 – The variation in mass versus time as a function of concentration for Ludox HS deposited onto a Silica QCM-D Crystal at pH 5 using the Q-Sense System.

4.3.3 Summary

The anionic silica particle Ludox HS has been shown to carry negative charges from pH 10 to pH 4. At these pH values the particle size, within error, is constant and no aggregation is observed. This implies that the double layer repulsive force remains sufficiently large to ensure electrostatic stabilisation of the particles. The material does not deposit onto a similarly charged silica QCM-D wafer at either pH 10 or pH 5 where the wafer will also carry negative charges due to ionised silanol groups.

4.4 Ludox CL Modified Silica

The cationic dispersion, Ludox CL, consists of silica particles modified by coating the surface with a layer of aluminium oxide[1]. The manufacturer details the surface structure to be a single layer of aluminium attached to oxide groups associated with silica with chloride as counterions. The measured thickness of this coating is approximately 5 nm and as such, this material behaves as alumina not silica. The material would be expected to carry a positive charge at low pH values, decreasing towards the isoelectric point at about pH 9 and the univalent chloride ions can be held at the surface by electrostatic

forces to balance the surface charges. However, there is some evidence that the counterions can also be bound onto the oxide surfaces[7] or form weak ion pairs with charged surface hydroxyl groups[8]. Commonly hydrated alumina surface is amphoteric in nature and is able to adsorb or release protons.

$AlOH + H^+ = AlOH_2^+$ (4.2)

$AlOH = AlO^- + H^+$ (4.3)

Under acidic conditions, pH <7, the surface would be positively charged as indicated by Equation 4.2. On addition of OH^- ions, equation 4.2 will be reversed and the surface will become more neutral and eventually at very high pH values will pass through the isoelectric point and become negatively charged[9]. The aluminium ion has high charge density and as such induces strong polarisation on the oxygen atom. This means that the bonds formed are intermediate in nature with both covalent and ionic character.

4.4.1 Solution Chemistry

As stated before, the pH range of interest for personal products is characteristically pH 4-7. Zeta potential measurements and particle size distributions were observed for the modified Ludox CL dispersion in this pH range.

4.4.1.1 Particle Dispersion Behaviour in the pH Range 4-7

An acid-base pH titration of the modified Ludox CL was performed from the natural pH to about pH 6 with no supporting electrolyte. The real interest in the deposition behaviour of these particles is limited to the pH range of 5-6 as this is the area in which the particles will be formulated. Figure 4.8 shows the alkali pH titration of Ludox CL with no electrolyte from pH 4 to pH 6 whilst Figure 4.9 shows the acid titration from pH 6 to pH 4. The zeta potential and particle size were evaluated and do not change, within experimental error, in this pH range. At this pH enough protons are present to ensure the surface is mostly $AlOH_2^+$ and thus the surface charge is highly positive. The electrical double layer repulsion forces are therefore high and the particles would not be expected to approach each other close enough for aggregation to occur. The pH titration

will introduce electrolyte into the system but not enough to reduce the electrical double layer or modify the diffusion coefficient significantly.

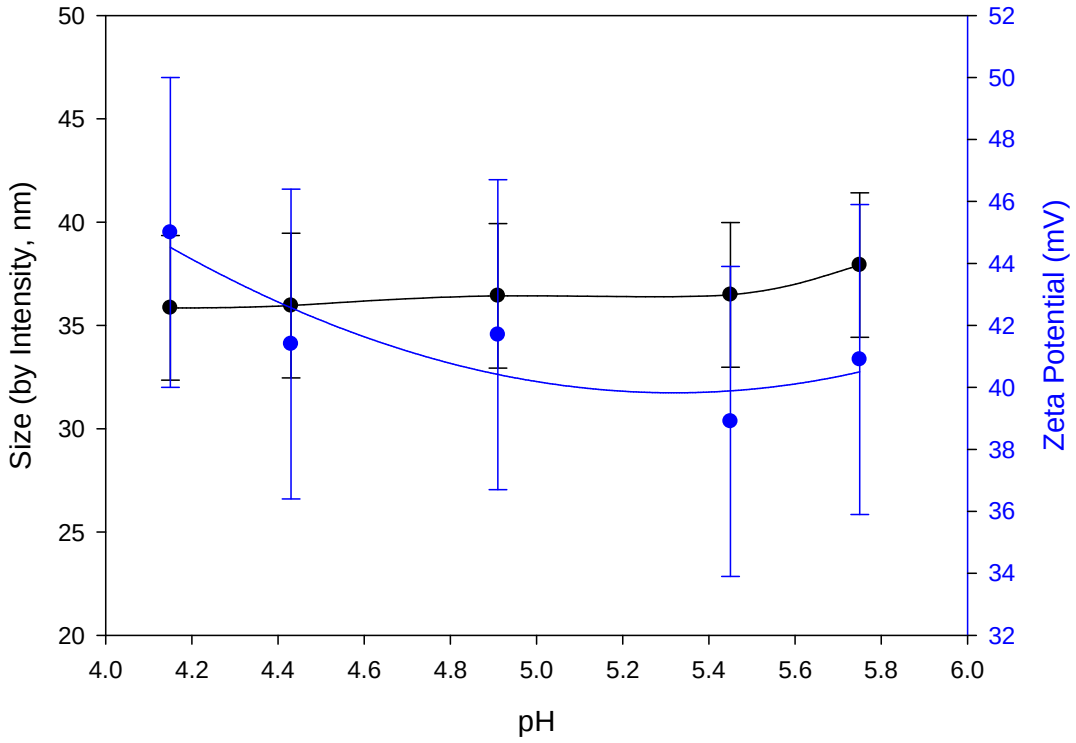

Figure 4.8 – The variation in intensity weighted particle size and Zeta potential data for modified silica Ludox CL when titrated against alkali from pH 4 to pH 6.

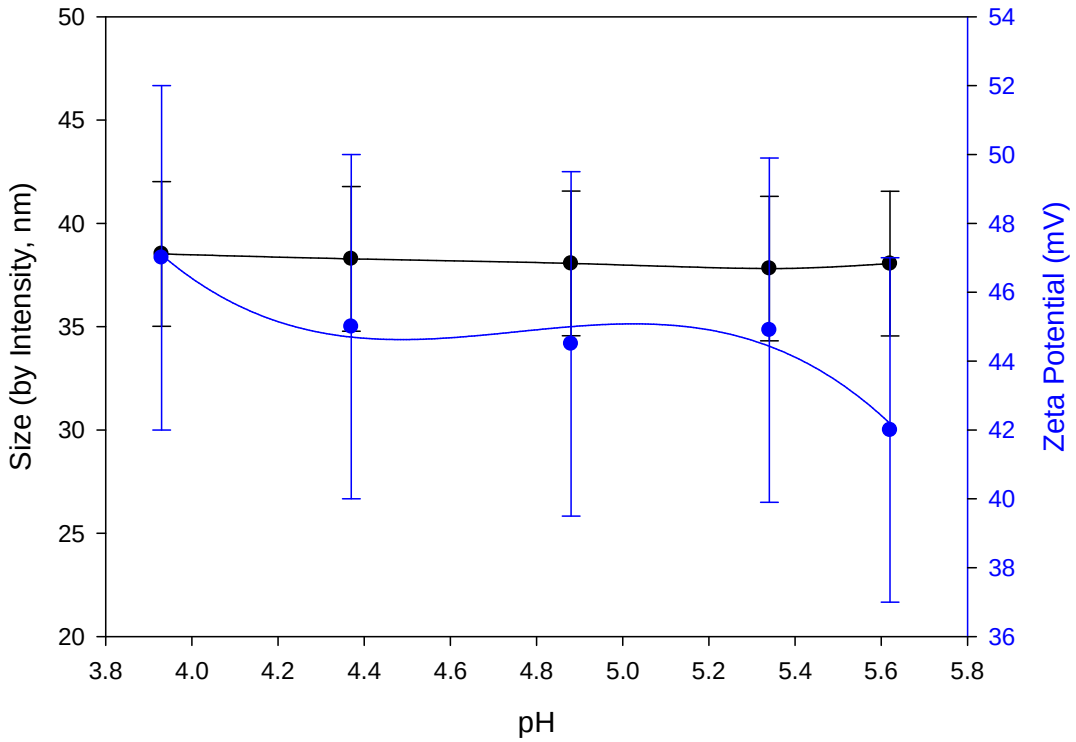

Figure 4.9 – The variation in intensity weighted particle size and Zeta potential data for modified silica Ludox CL when titrated against acid from pH 6 to pH 4.

4.4.1.2 Particle Dispersion Behaviour in Other pH Ranges

It is worthwhile to explore the behaviour of this material as it approaches its isoelectric point, in order to better understand any variations seen at lower pH ranges due to the coating. Therefore, an acid-alkali pH titration was performed from pH 3 to pH 9 and then reversed. Figure 4.10 shows the variation in zeta potential and intensity weighted particle size distribution for the alkali titration from pH 3 to pH 10 for Ludox CL whilst Figure 4.11 shows the same data for the reverse acid titration from pH 10 to pH 3.

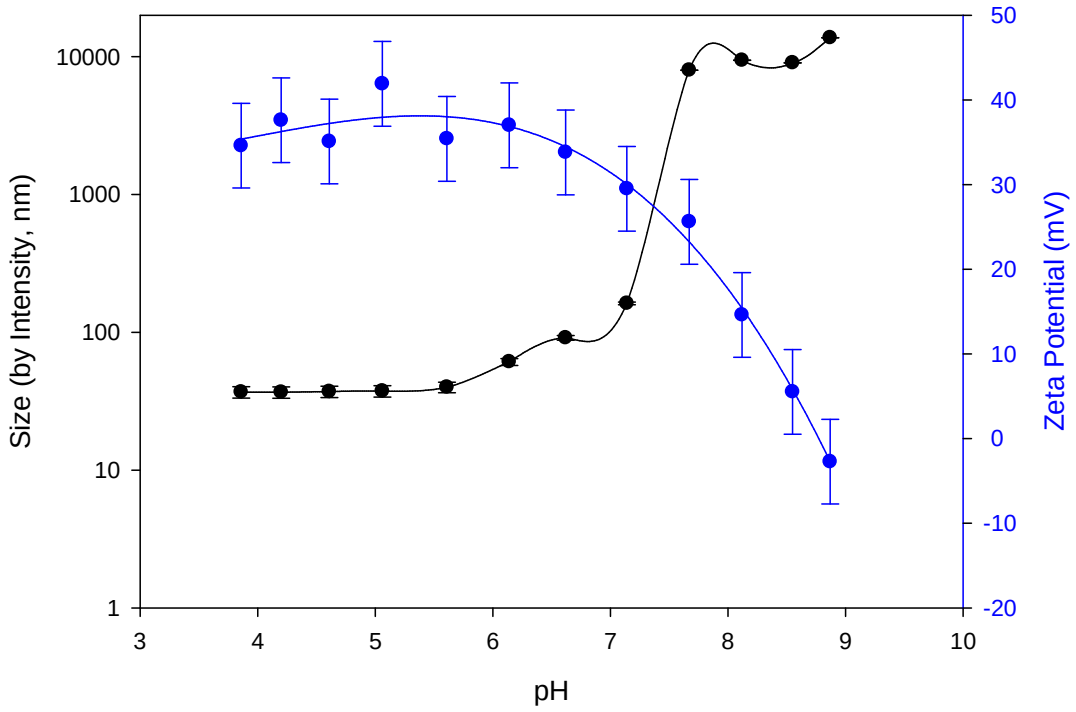

Figure 4.10 – The variation in intensity weighted particle size and Zeta potential data for modified silica Ludox CL titrated against alkali from pH 3 to pH 9.

As the material approaches pH 7, the zeta potential begins to decrease finally passing through the isoelectric point at a value of approximately 8.7. This is in agreement with literature values of about 9.0 for various alumina samples with different electrolyte types and concentrations[10,11,12]. This coincides with a huge increase in particle size as the material aggregates, changing from 40 nm to greater than 1 micron, which is the upper limit for the technique, in agreement with similar behaviour noted for α-alumina samples[13]. When the pH is reversed, in Figure 4.11, the zeta potential recovers as seen previously with the Ludox HS silica but the particles do not regain their original size range and remain as aggregates of approximately 1 micron. As the pH is increased, the electrostatic repulsion between the particles is reduced due to the neutralisation of the charge at the particle surface. This allows the particles to closely approach one another and aggregation occurs[14]. This is commonly measured as coagulation or sedimentation[10,13]. It should be noted that aggregation occurs before the isoelectric point is reached. The primary minimum could be approached as this depends upon the 1/κ distance. Depending upon the depth of the attractive potential well, upon restoration of

the electrostatic repulsion, some of the particles may remain as larger aggregates. Others may only be flocculated in a weak secondary minimum and can redisperse.

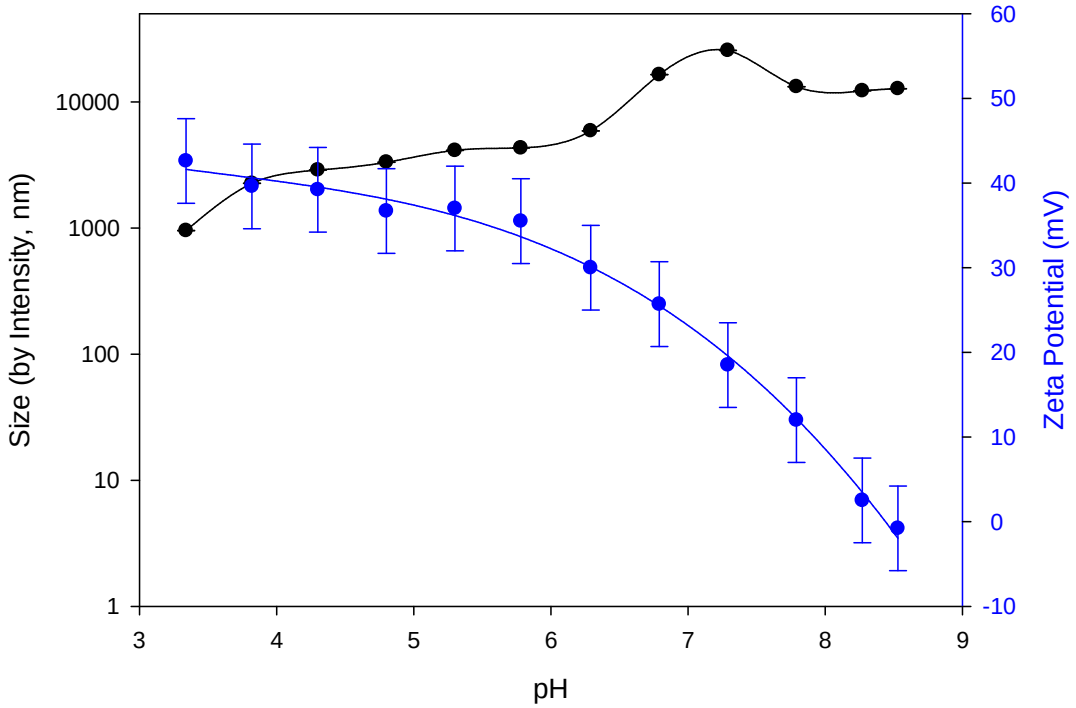

Figure 4.11 – The variation in intensity weighted particle size and Zeta potential data for modified silica Ludox CL titrated against acid from pH 9 to pH 3.

4.4.2 Addition of Indifferent Electrolyte

All the previous measurements were performed with no added electrolyte in the system. The amount of electrolyte generated by the large titrations of acid and base to modify pH varied could have an effect on the system. The amount of electrolyte generated by the addition of acid and base was calculated as follows:

$pH = -\log[H^+]$ at values <7

$pH = 14-\log[OH^-]$ at values >7

For H^+,

At pH 3 the concentration is $1x10^{-3}M$

At pH 4 the concentration is $1x10^{-4}M$

At pH 5 the concentration is $1x10^{-5}M$

At pH 6 the concentration is $1x10^{-6}M$

At pH 7 the concentration is $1x10^{-7}M$

For OH^-,

At pH 7 the concentration is $1x10^{-7}M$

At pH 8 the concentration is $1x10^{-6}M$

At pH 9 the concentration is $1x10^{-5}M$

The maximum electrolyte concentration is approximately $2.02x10^{-3}M$.

An inert electrolyte value of 0.01M NaCl was chosen as this would buffer the acid-base values and allow for a constant electrolyte level in the system. Since the changes in electrolyte induced little change in the Ludox HS dispersion behaviour, only the titrations for Ludox CL were repeated.

First, titrations of Ludox CL were performed against increasing NaCl. This was to ensure that the chosen level of electrolyte would not adversely affect the material behaviour by totally suppressing the electrostatics in the system. Figure 4.12 shows the changes in zeta potential and intensity particle size distribution on titration of increasing levels of NaCl against Ludox CL.

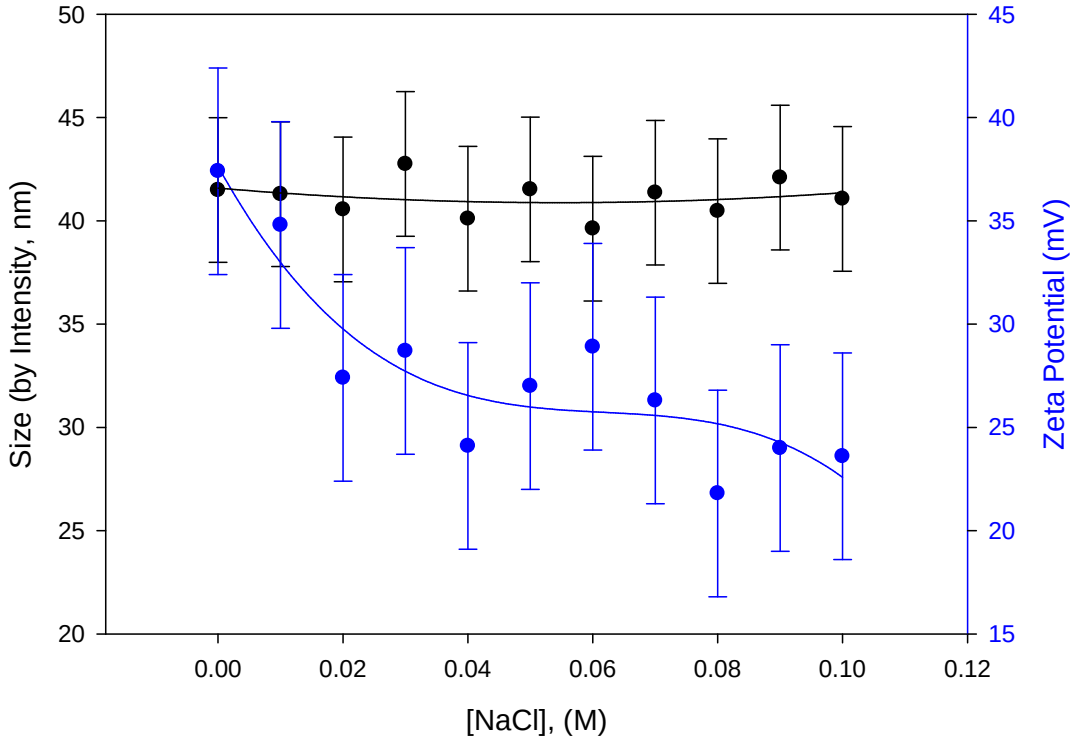

Figure 4.12 – Intensity weighted particle size and Zeta potential values for modified silica Ludox CL titrated against increasing NaCl.

The addition of 0.01M NaCl manifests some influence on the zeta potential but at 0.02M and above, the effect on the electrokinetic properties becomes significant, shown by a reduction in zeta potential from approximately 40mV to 30mV. A level of 0.01M is therefore considered low enough for the system to be studied.

4.4.2.1 Dispersion Behaviour at pH Range 4-7 with Indifferent Electrolyte

Figure 4.13 shows the particle size and zeta potential data for the base pH titration of Ludox CL from 4 to 6 with 0.01M NaCl whilst Figure 4.14 shows the reverse acid titration from 6 to 4. The zeta potential remains constant in both directions as does the particle size. This is equivalent to the data obtained for this pH range with no electrolyte and illustrates that the electrolyte amount generated in this titration does not radically affect the particle behaviour.

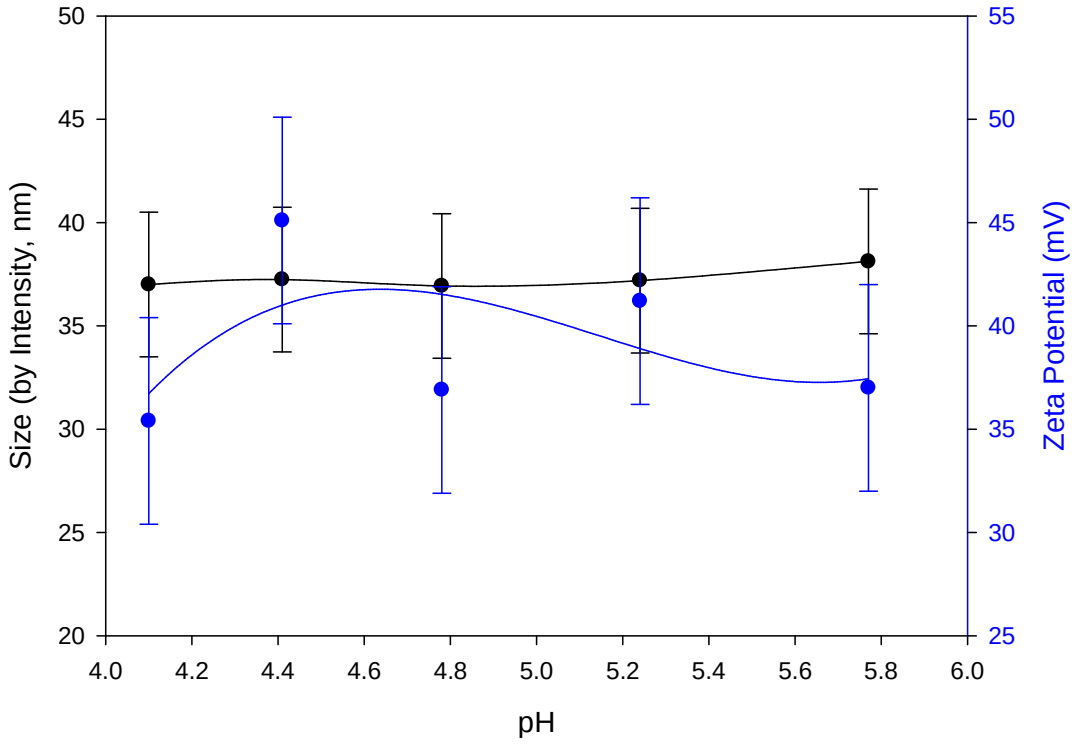

Figure 4.13 – The effect of varying the dispersion pH from 4 to 6 on the intensity weighted particle size and zeta potential data for modified silica Ludox CL, in the presence of 0.01M NaCl.

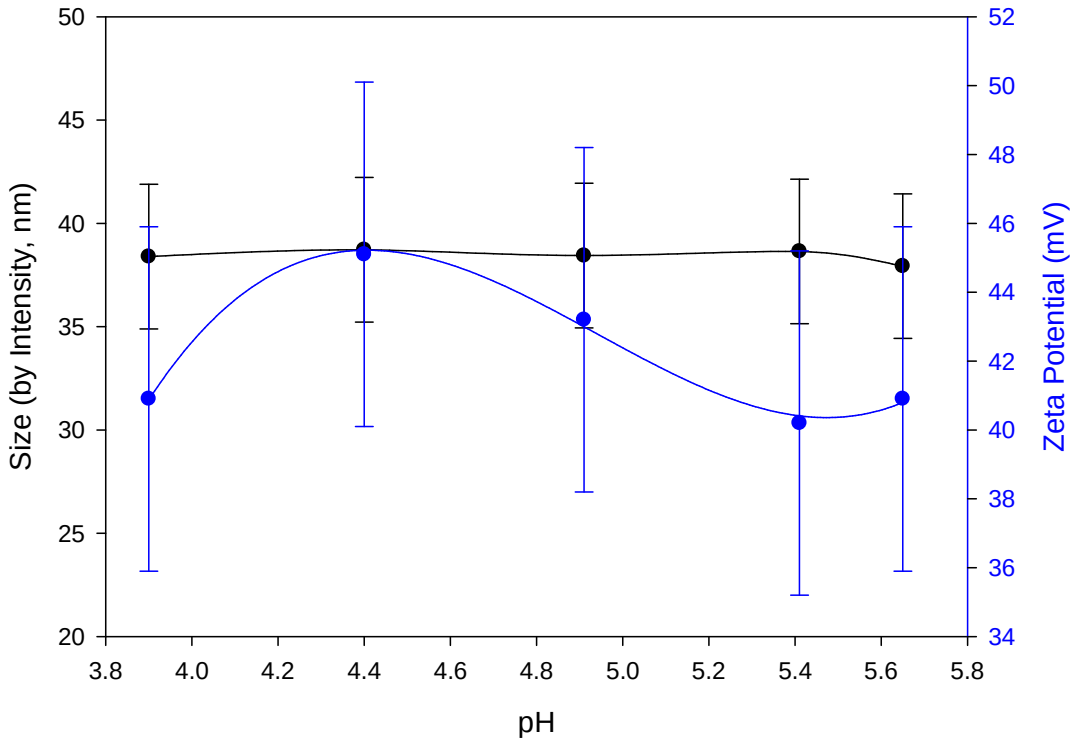

Figure 4.14 – The effect of varying the dispersion pH from 6 to 4 on the intensity weighted particle size and zeta potential data for modified silica Ludox CL, in the presence of 0.01M NaCl.

4.4.2.2 Dispersion Behaviour in Other pH Ranges

When the pH 4 to 9 acid-base titrations are repeated in indifferent electrolyte, similar results are obtained. Figure 4.15 shows zeta potential and intensity weighted particle size distributions for the base titration from pH 4 to 9 and Figure 4.16 shows the zeta potential and intensity weighted particle size distributions for the reverse acid titration from pH 9 to 4. The zeta potential begins to decrease around pH 7-8 and particle growth is seen accordingly as the double layer repulsion is reduced and the particles are destabilised. The zeta potential is able to recover to the original value indicating that the protons can still interact with the alumina surface and allow electrostatic charges to develop. Due to the increase in electrostatic potential the particles are able to disaggregate and recover to approximately 150 nm instead of the 1 micron seen

previously with no electrolyte. This indicates that the particles are not as strongly aggregated as seen previously. According to the DVLO theory, addition of electrolyte causes a reduction in the range of the electrostatic repulsive force between the particles which allows for closer approach of the particles[15] producing a secondary minimum where a weak, reversible adhesion between particles can exist. The particles can then be broken up by applying shear as in this example. Gentle shaking of the dispersion however is not sufficient to break up aggregates smaller than 100nm and primary particle size is not recovered.

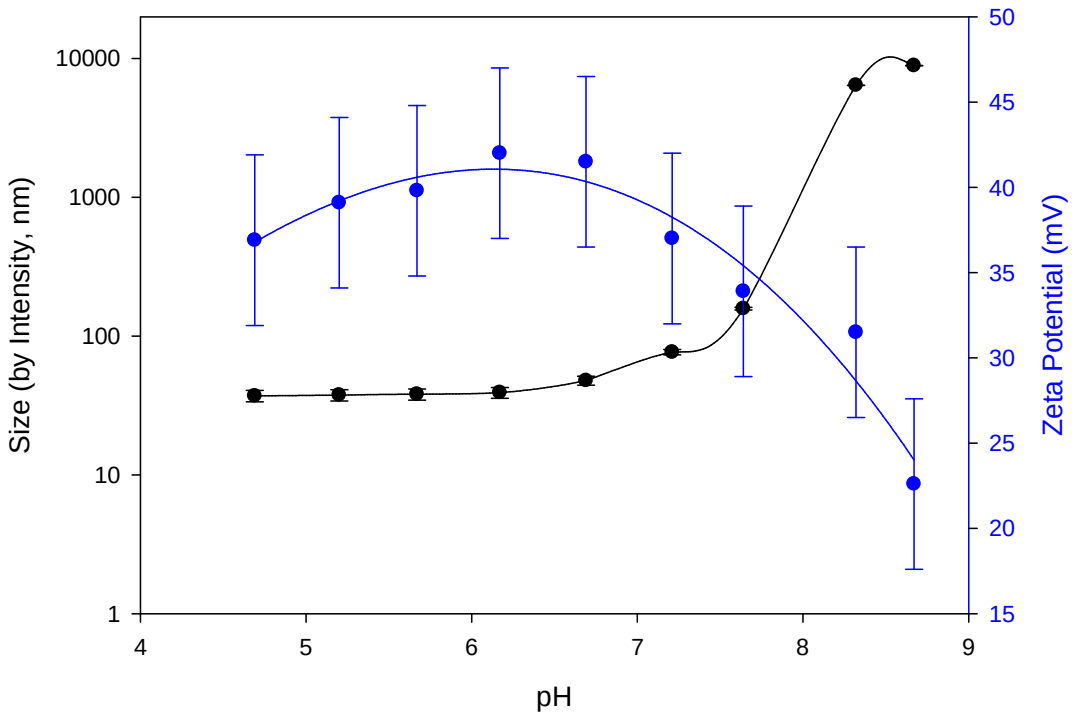

Figure 4.15 – The effect of varying the dispersion pH from 4 to 9 on the intensity weighted particle size and zeta potential data for modified silica Ludox CL, in the presence of 0.01M NaCl.

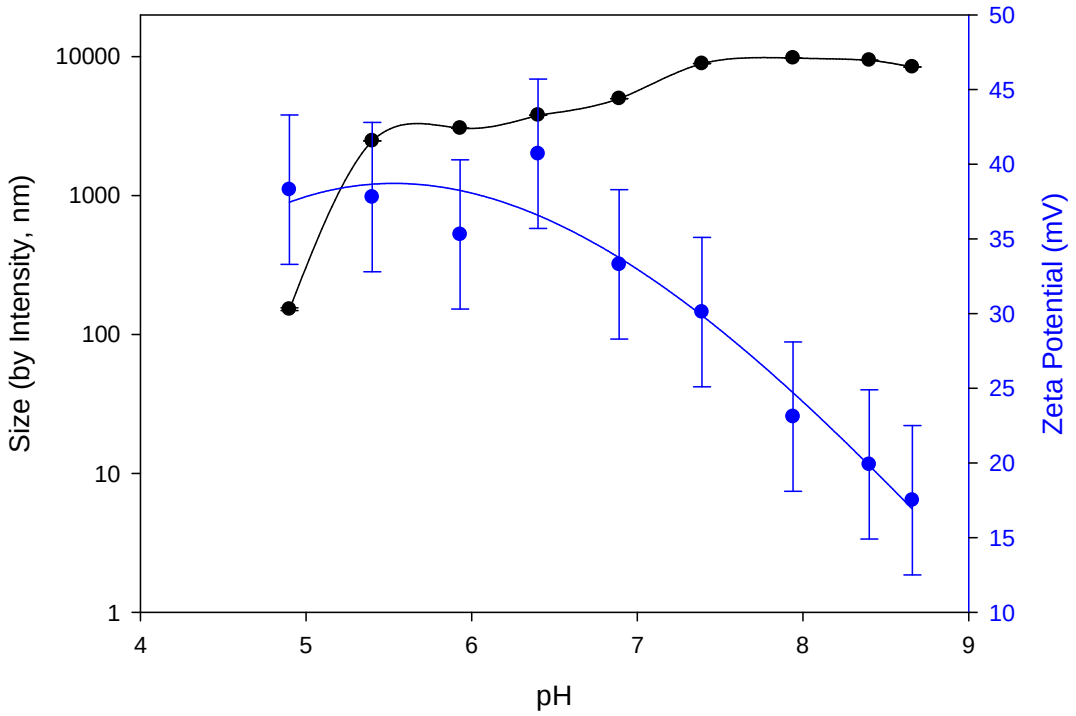

Figure 4.16 – The effect of varying the dispersion pH from 9 to 4 on the intensity weighted particle size and zeta potential data for modified silica Ludox CL, in the presence of 0.01M NaCl.

4.4.3 Deposition onto Surfaces

4.4.3.1 Quartz Crystal Microbalance

In order to complement the dynamic light scattering and the electrokinetic property measurements, deposition characterisation experiments were performed by means of a quartz crystal microbalance. The experimental set-up is discussed previously in section 4.3.2.1.

In all cases, plain silica surfaces were used as the hydrophilic substrate. Silica, as discussed previously, carries negative electrostatic charges in the pH range of interest. The silica substrate used was similar to that previously shown in Figure 4.7 and the bare oxide surface results looked the same.

Measurements were performed on the modified silica at three concentration levels and at pH 3-4 (natural pH) and 5 (pH of interest). The concentrations of material for this experiment were limited by the sensitivity of the technique[6].

4.4.3.1.1 Ludox CL Deposited at pH 3-4 (Natural pH)

The modified silica particles carry a positive charge and would be expected to deposit strongly onto the QCM crystal. As the concentration of material in the dispersion increases, more would be expected to deposit; assuming diffusion is influencing the particle behaviour. Figure 4.17 shows the final amounts of Ludox CL deposited onto a QCM silica wafer at pH 3 with no electrolyte under both quasi-diffusion (KSV apparatus) and diffusion/convection (Q-sense device) systems. For the diffusion system, only the particles contained in the sample could deposit during the lifetime of the experiment whilst for the convection experiment, due to the flow, particles are constantly brought into contact with the surface and also removed if they do not adhere strongly.

The quasi-diffusion method clearly shows that the final amount of deposited silica increases with the concentration of silica in dispersion. However, the convection experiment shows similar final values for all concentrations. Since deposition and removal are occurring simultaneously, despite the different starting levels, the material eventually reaches equilibrium with the surface, although this can take up to 20 hours.

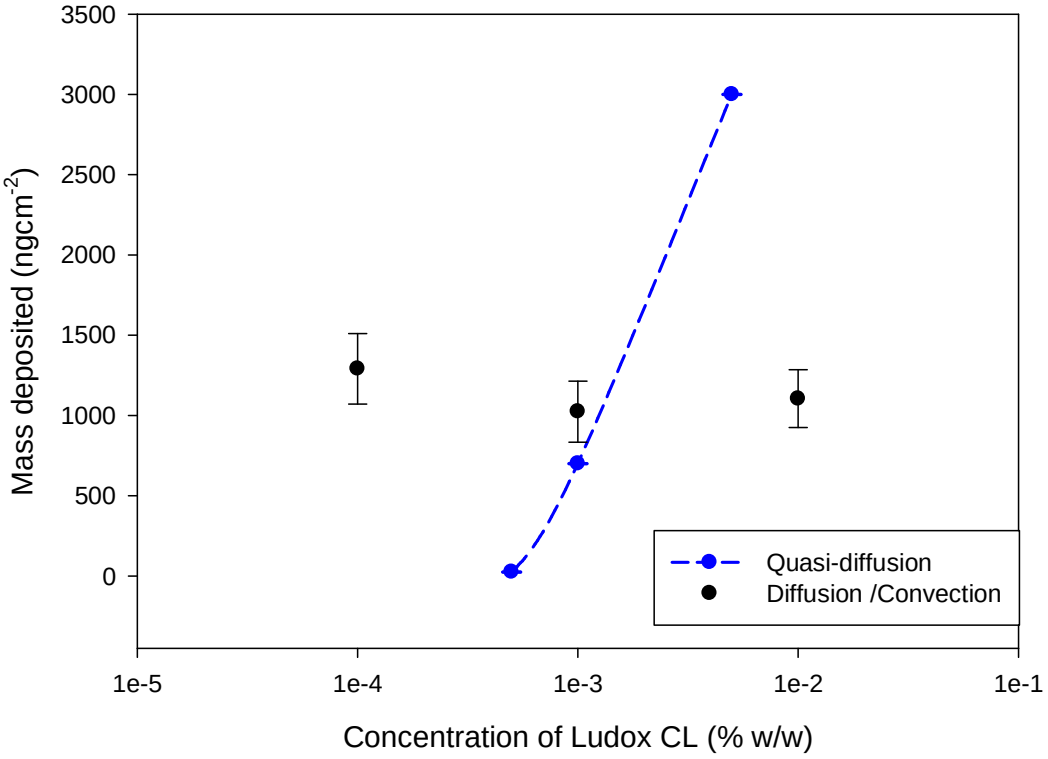

Figure 4.17 – Final Ludox CL levels deposited onto silica QCM-D crystals at pH 3 in the absence of background electrolyte.

At this pH value, the crystal silica surface is close to the isoelectric point and is not highly charged but there should still be some electrostatic attraction between the Ludox CL particles and the surface. In the quasi-diffusion system, only the number of particles in the sample can deposit on the surface as there is no flux to remove them hence increasing concentration results in increasing deposition. In the diffusion/convection system, there is no reason for the particles to remain stuck to the crystal silica surface and the particles are able to be removed until equilibrium between the deposition and removal of particles is obtained leading to similar deposition amounts for all concentrations.

An initial high rate of deposition is seen at high concentrations of Ludox CL due to the number of collisions between the bare surface and the particles. However, as stated above, there is little reason for the particles to remain on the silica surface and they are removed with flux. It is possible that there could also be some slow leaching of

aluminium ions at this pH which slowly change the surface charge leading to subsequent particles that contact the surface being repelled and unable to stick and leading to equivalent final values.

4.4.3.1.2 Ludox CL Deposited at pH 5-6

At pH 5, totally different behaviour is observed. Figure 4.18 shows the maximum Ludox CL deposited onto a QCM silica wafer at pH 5 in the absence of indifferent electrolyte. Unexpectedly, as the concentration of Ludox CL in the dispersion increases, the amount deposited decreases. Zeta potential measurements have shown that the material has a high positive charge at pH 5 (see Figure 4.7) and the QCM crystal surface is negatively charged due to ionisation of silanol surface sites so the material would be expected to deposit strongly. Both the diffusion and convection experiments show the same trends and repeat measurements are reproducible within experimental error. The higher the particle concentration in the system, the larger the amount of electrolyte produced, however conductivity experiments show that the amount of electrolyte produced by these concentration values is insufficient to screen charges and modify the deposition.

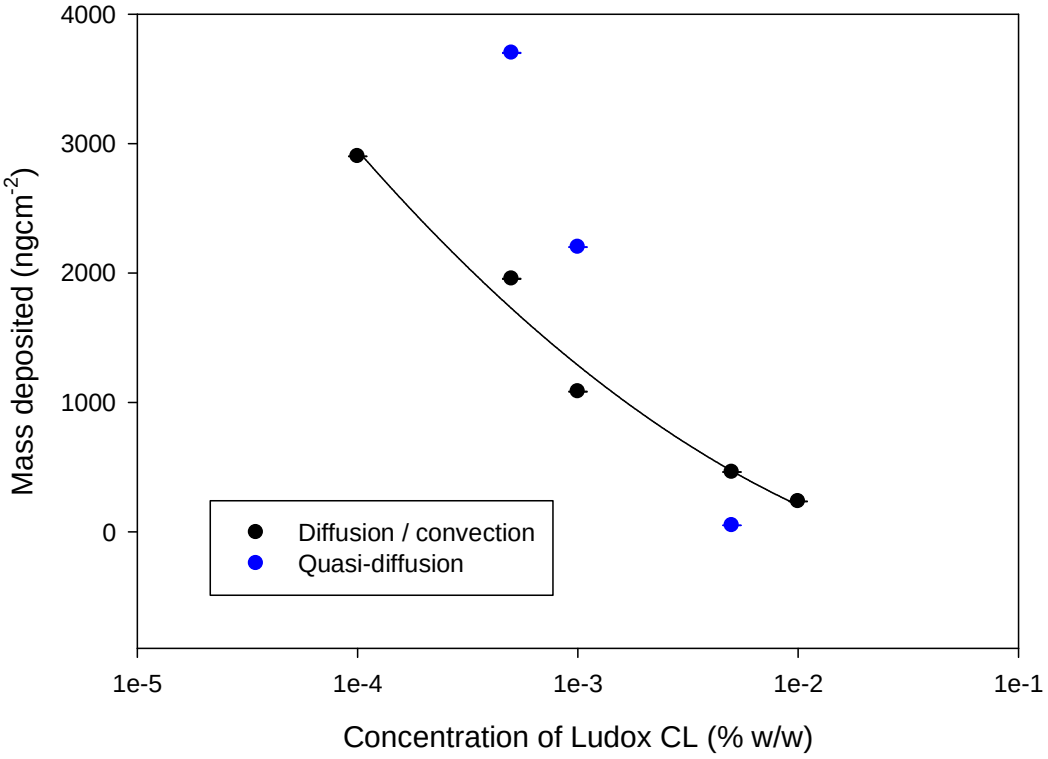

Figure 4.18 - Final Ludox CL levels deposited onto silica QCM-D crystals at pH 5 in the absence of background electrolyte

Figure 4.19 shows the deposition profile of Ludox CL at pH 5 onto silica QCM crystals using the Q-Sense diffusion/convection machine. This time, there is no removal of the surface bound silica as the maximum amount deposited remains the same even after the experiment is allowed to run for 21 hours. Here, at the higher concentrations, Ludox CL goes down quickly to the substrate surface but very little remains adhered.

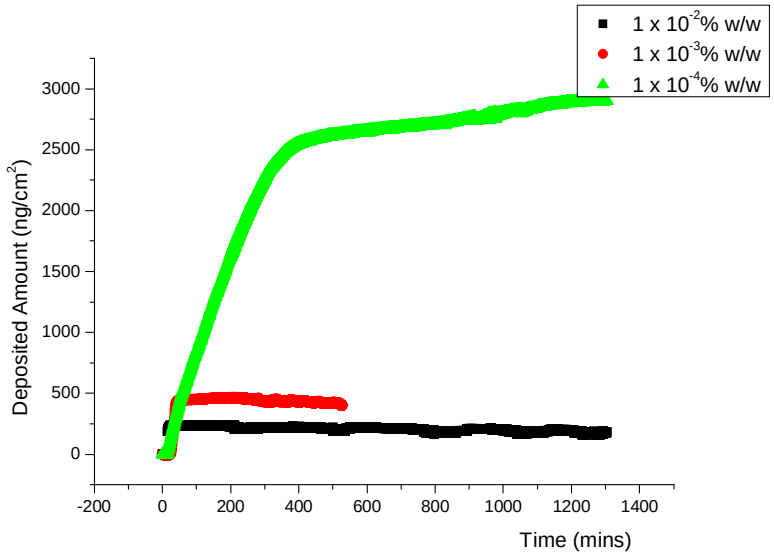

Figure 4.19 - Ludox CL Deposition Profiles onto silica QCM-D crystals at pH 5 in the absence of background electrolyte

Deposition profiles of latices onto mica surfaces have been studied using the oblique impinging jet cell[16] which allows the deposition rates to be modelled as the stagnation point can be determined by visual observation of particle trajectories and the fluid velocity field calculated using the Navier-Stokes equation. Deposition rates are shown to be dependent upon the time and concentration of dispersion. Since we are using QCM-D, we are unable to quantify the hydrodynamics within the flow chamber hence no modelling of the deposition rates was possible. Layer by layer deposition of silica particles onto gold surface[17] has been performed by recharging the deposited silica layer between each dip into silica dispersion but no flow was present and changes seen in deposited particle density are mainly attributed to electrostatic screening.

It can be seen that, in our system, the lower concentrations of Ludox CL deposit at a slower rate but to a much greater degree. As the particle surface properties do not change significantly between pH 3 and 5, it appears that the deposition of the particles at higher concentrations is retarded by something present on the surface. The reason for this is going to be considered in the following discussion section.

The crystal silica surface is highly negatively charged at pH 5 and since the particles carry positive charges, there is strong electrostatic interaction. Due to this interaction, once the particles are in contact with the surface they are very unlikely to detach and this is seen in the deposition profiles. At higher concentrations Ludox CL would be expected to deposit more quickly due to the higher number of collisions between the particles and the silica surface and this is also observed in the deposition profiles. However, the final deposited amount is reduced with increasing concentration of particles and we will refer to this more in the discussion.

4.4.4 SEM Images of Deposited Ludox CL Modified Silica Particles

In order to visualise the phenomena, scanning electron micrographs were taken of the Ludox CL modified particles on the surface of the QCM crystal. Crystals used on the quasi-diffusion KSV machine were allowed to dry naturally once the experiment was completed before visualisation. Drying could introduce artefacts in the deposited films due to capillary bridging between the particles[18] but the sizes of the particles in the images are in agreement with the data obtained from particle size experiments.

4.4.4.1 SEM Images at pH 3

Figures 4.20 to 4.22 show the Ludox CL particles at decreasing dispersion concentrations at pH 3. Here, the quasi-diffusion experiment shows a decrease in the number of particles initially adhering to the substrate but the convection experiment shows equivalent numbers. The images do show some decreasing particle numbers as these were obtained from the static deposition experiment. It can also be noted that the particles are deposited as aggregates of 100nm which appear to be further aggregated although this may be an artefact due to aggregation driven by capillary forces[18].

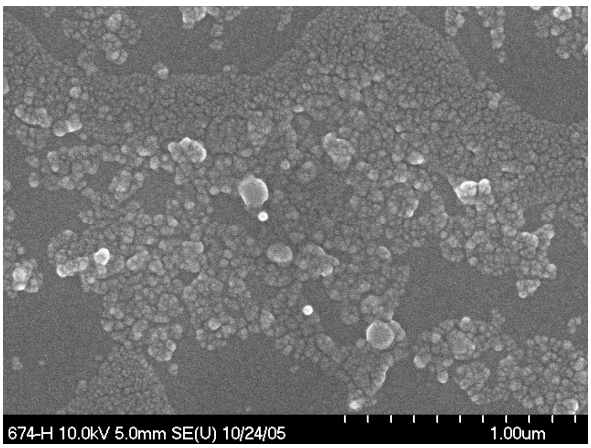

Figure 4.20 – SEM image of a dried film of $5x10^{-3}$% w/w Ludox CL at pH 3 deposited onto a QCM silica crystal.

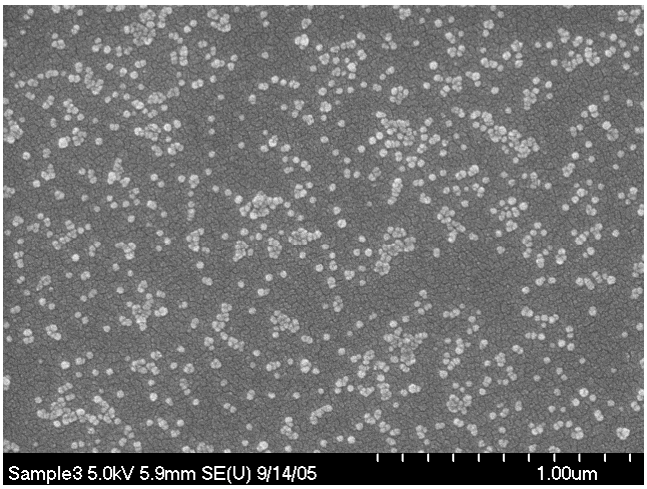

Figure 4.21 – SEM image of a dried film of $1x10^{-3}$% w/w Ludox CL at pH 3 deposited onto a QCM silica crystal.

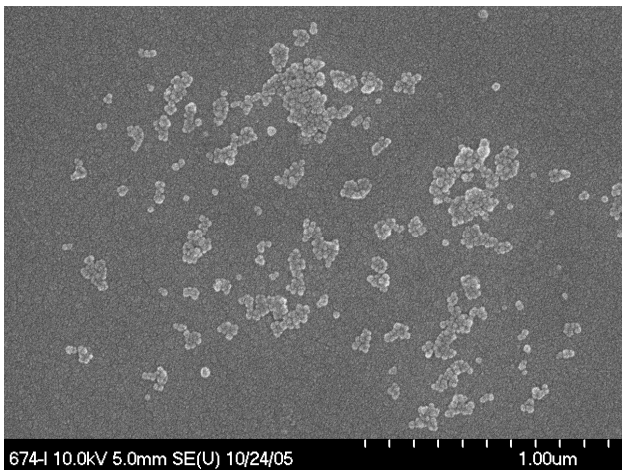

Figure 4.22 – SEM image of a dried film of $5x10^{-4}$% w/w Ludox CL at pH 3 deposited onto a QCM silica crystal.

4.4.4.2 SEM Images at pH 5

Figures 4.23 to 4.25 show surface Ludox CL particles with decreasing particle dispersion concentrations at pH 5. Here, the QCM detects an increase in the number of deposited particles and this is clearly shown in the images. It can also be noted that discrete spheres are observed on the surface but each is of the order of 100nm. This is larger than the size of an individual silica particle and suggests that the particles might deposit as aggregates, trimers or tetramers. The larger secondary aggregates seen at pH 3 do not appear.

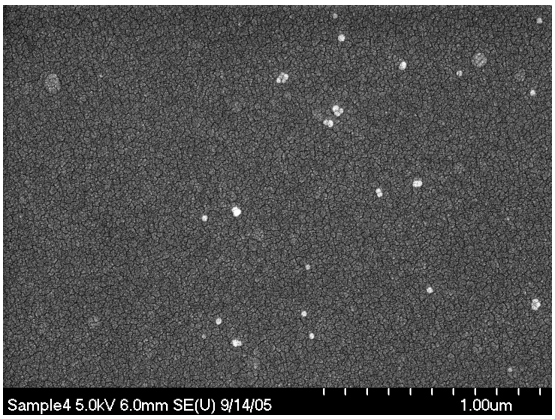

Figure 4.23 – SEM image of a dried film of $5x10^{-3}$%w/w Ludox CL at pH 5 deposited onto a QCM silica crystal.

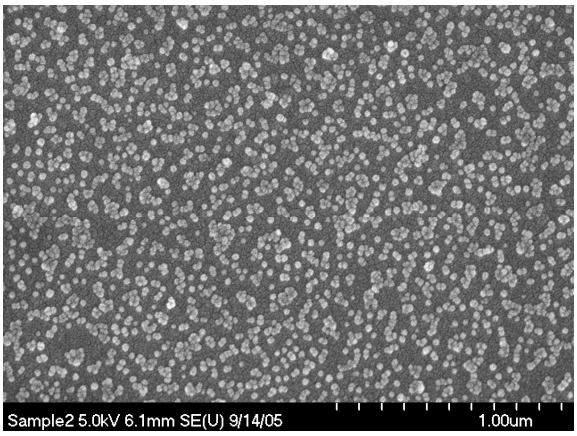

Figure 4.24 – SEM image of a dried film of $1x10^{-3}$% w/w Ludox CL at pH 5 deposited onto a QCM silica crystal.

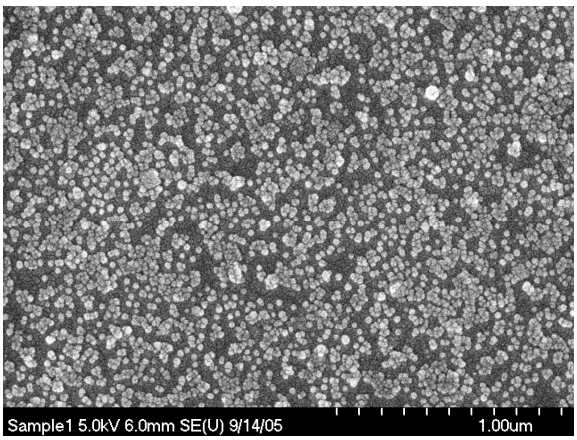

Figure 4.25 – SEM image of a dried film of $5x10^{-4}$% w/w Ludox CL at pH 5 deposited onto a QCM silica crystal.

4.4.5 Discussion

Since the Ludox CL material is cationic and would be expected to adhere strongly to the substrate at pH 5, it appears that something is present on the substrate at this pH that prevents the deposition of the modified silica particles. Since the substrate is identical in each case, and at pH 5 is negatively charged, the change to the surface must be

delivered from the silica dispersion. As like charges repel, a possible explanation is that the aluminium coating on the Ludox particles is dissolving and releasing ions which adsorb at the silica surface and reverse the charge. The effect would be more dramatic at the higher concentrations as the rate of aluminium leaching would scale with particle number density. Calculations based on ionic radii show that ionic diffusion would lead to free ions meeting the surface far more quickly than the CL particles.

A quick evaluation based on the Stokes-Einstein equation clearly demonstrates the differences in the diffusion rates. Using Equation 2.2, particle diffusion coefficients can be derived.

Assuming the viscosity of the dilute solution is close to water and the temperature is 300 K then:

For a 20nm silica particle D is 1.1×10^{-11} $m^2 s^{-1}$

For a 53.5pm aluminium ion D is 4.1×10^{-9} $m^2 s^{-1}$

This calculation does not take into account the hydration shell of the ion but quoted values[19] range from 0.8-1x $10^{-10} m^2 s^{-1}$.

4.4.6 Identification of the Presence of Aluminium ions

In order to verify the hypothesis and confirm that aluminium ions were being released by the particles, a 1% dispersion of Ludox CL was placed into a 3000 Da molecular weight cut-off dialysis bag. This was stirred gently in 100ml of distilled water for 24 hours so the total concentration of Ludox CL would be 1×10^{-3} wt%. The diluent was then analysed by NMR for the presence of aluminium[20]. Figure 4.26 shows the NMR ^{27}Al spectrum produced for the Ludox CL diluent.

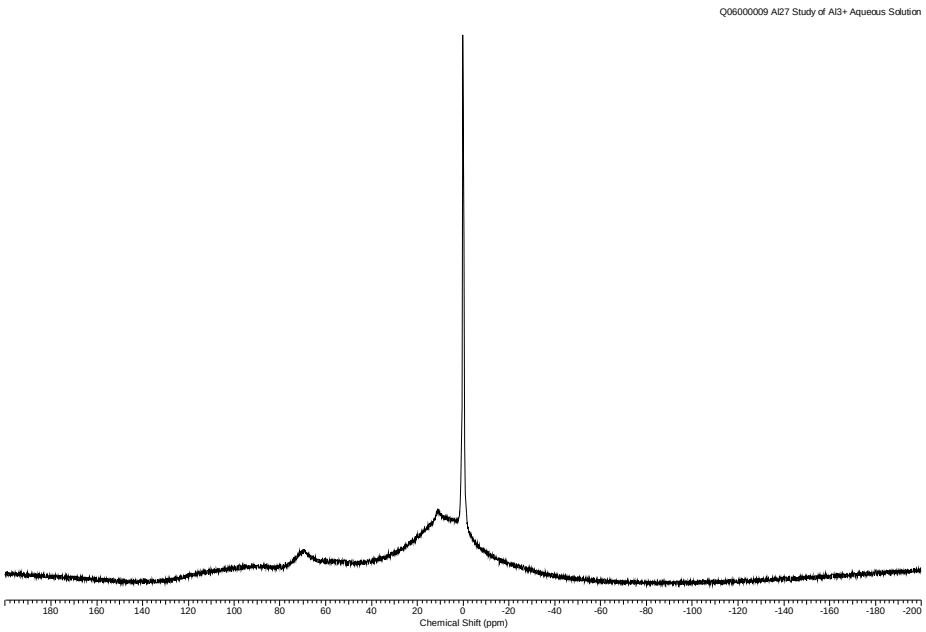

Figure 4.26 – ^{27}Al NMR Spectra of Solution Obtained from Dialysis of Ludox CL

A sharp peak at 0ppm can be observed which is assigned to Al^{3+}. Broader polymeric type signals can also be observed which are typical for tetrahedral and octahedral ^{27}Al environments. These are probably due to breakdown of the aluminium oxide coating on the particle. All shifts are with respect to a sodium aluminate standard.

4.4.7 Estimation of Aluminium Concentration

To try and calculate the concentration of aluminium ions released, the conductivity of the diluent solution was measured and compared to a calibration curve. Figure 4.27 shows the calibration curve for sodium and aluminium chloride. The conductivity was found to be equivalent to that of $1x10^{-5}$M aluminium chloride.

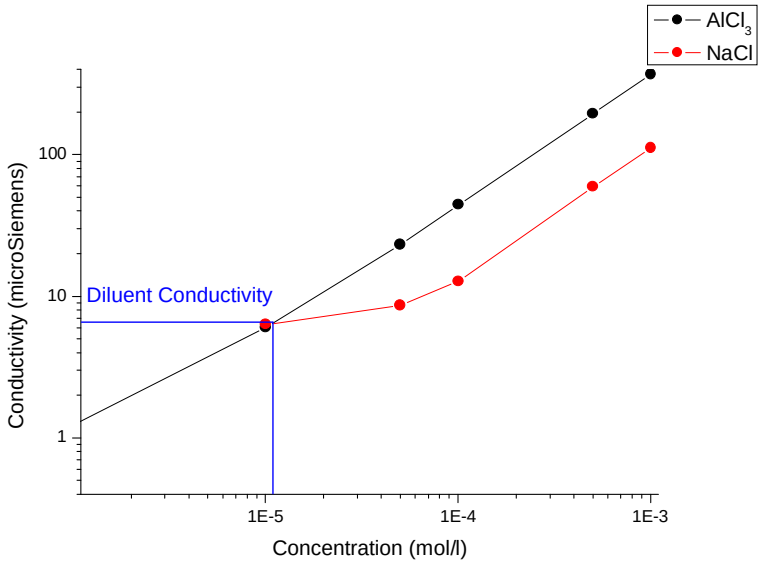

Figure 4.27 – Conductivity Calibration Curves for Aluminium Chloride and Sodium Chloride as a function of concentration.

4.4.8 Streaming Potential of Silica Wafers with Aluminium Ions

To determine what effect this concentration of aluminium ions would have on the substrate, streaming potential measurements were performed on a silica wafer. Figure 4.28 shows the streaming potential values at pH 3 and 5 both before and after addition of $1x10^{-5}$M aluminium chloride solution. Measurements were taken at both pH values using water only then a solution of $1x10^{-5}$M aluminium chloride was streamed over the wafer. Finally, the streaming potential was again measured at both pH values with water.

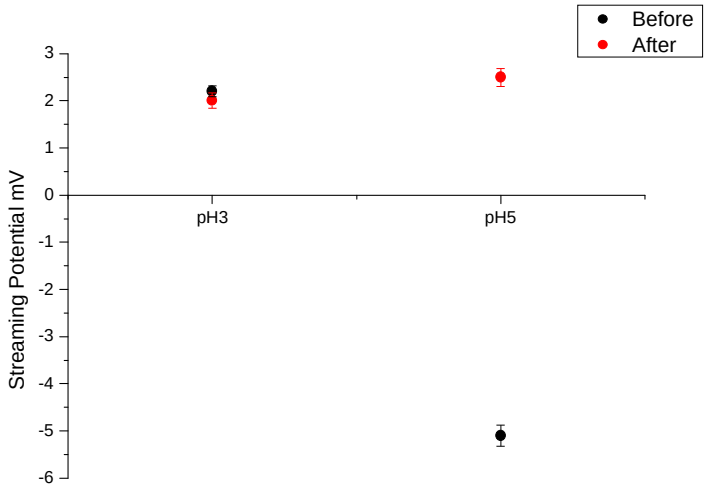

Figure 4.28 – Streaming potential values of silica wafers before and after addition of Aluminium Chloride solution.

The streaming potential measurements of a silica wafer were consistent with those obtained previously[5] on the same machine at Unilever Research with the isoelectric point measured at approximately pH 4. In this case, the streaming potential remained constant at approximately 2 mV at pH 3 however, at pH 5 it changed from -5mV to +2.5mV. This indicates that the level of aluminium leached from the Ludox CL dispersion at pH 5 is capable of changing the surface potential of the substrate.

4.4.9 Adsorption of Aluminium Ions onto QCM-D Crystals

To determine if this amount of aluminium ions could actually prevent deposition of the modified silica Ludox CL onto a QCM crystal, a $1x10^{-5}$M solution of aluminium chloride was flowed over a silica QCM crystal and the adsorption profile measured. A $5x10^{-3}$% Ludox CL suspension at pH 3 was added afterwards, which had been previously shown to significantly deposit, and the profile observed. Figure 4.29 shows an initial adsorption of aluminium ions onto the crystal surface. Once this has reached equilibrium and the Ludox CL is added the deposited mass remains constant. No

deposition of Ludox CL occurs when aluminium ions are already present on the substrate surface.

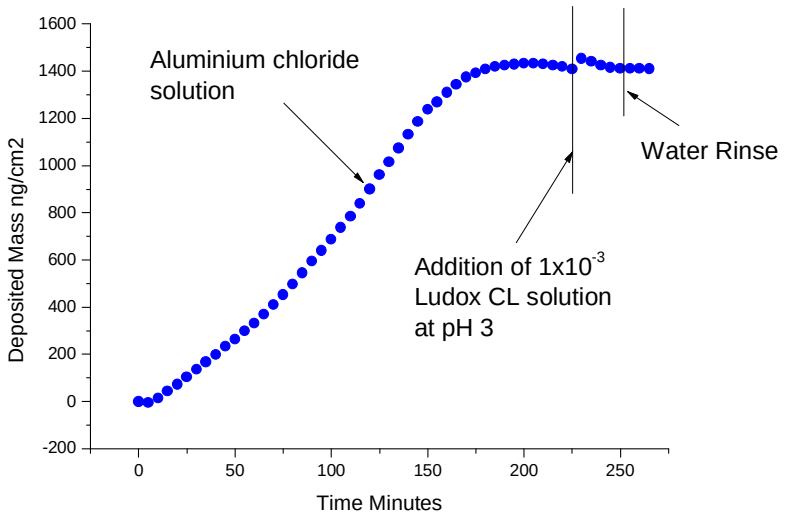

Figure 4.29 – Adsorption of Aluminium Chloride to a silica QCM-D crystal followed by deposition of modified silica Ludox CL.

4.4.10 DSIMS Analysis of Silica Wafers with Aluminium Ions

Further confirmatory evidence was obtained by probing the surface of aluminium contaminated wafers. DSIMS can be used to evaluate the level and depth of aluminium present on a substrate surface. Silica wafers were soaked in either distilled water (reference) or $1x10^{-5}$M aluminium chloride solution for 12 hours. They were dried and submitted for analysis for aluminium. Figure 4.30 shows the depth profile for silica and aluminium on the reference silica wafer and almost no aluminium is present. Figure 4.31 shows the depth profile for silica and aluminium on the wafer exposed to $1x10^{-5}$M aluminium chloride. This shows that there is 100 times more aluminium present on the surface and it covers the surface to a depth of 100 nm. It should be noted that this wafer is exposed to an aluminium chloride solution equivalent to that released by Ludox CL but no Ludox is present, so no competing deposition.

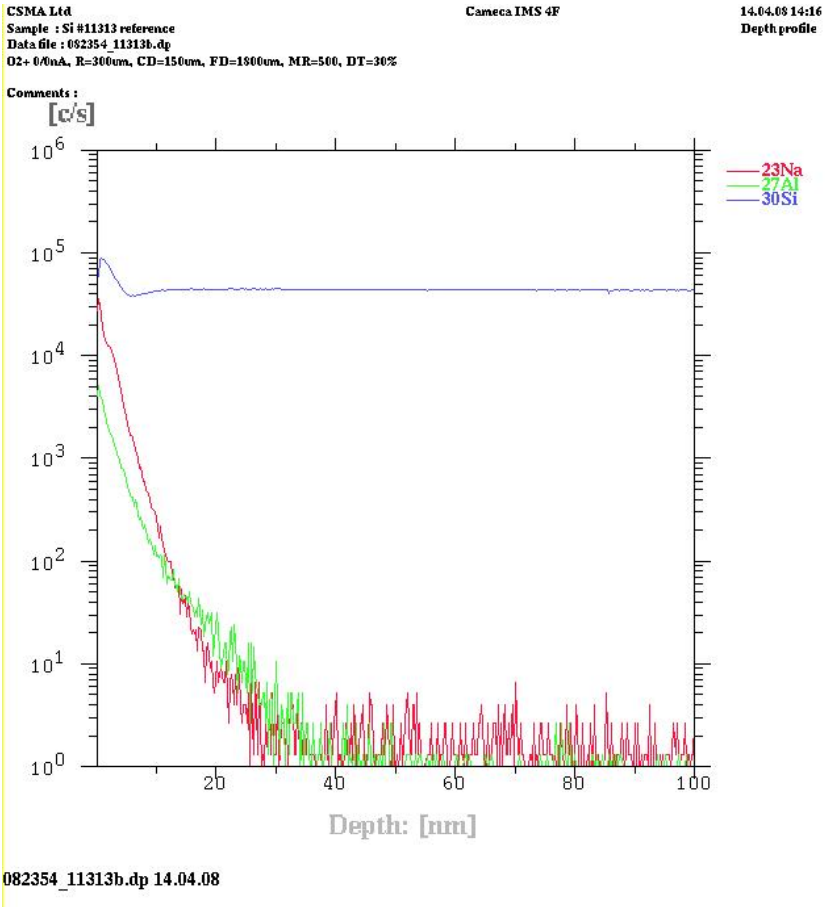

Figure 4.30 – DSIMS analysis of a plain silica reference wafer. Concentration of each material is shown at increasing depth in the sample.

These additional measurements utilising a series of techniques show that aluminium ions are released by the Ludox CL particle dispersion at pH 5. Streaming potential measurements indicate that the aluminium ions change the charge of the silica substrate and QCM measurements show the presence of aluminium ions retards deposition of the Ludox CL particles. Finally, DSIMS shows that the aluminium ions are present on the surface in vast quantities as a relatively thick layer.

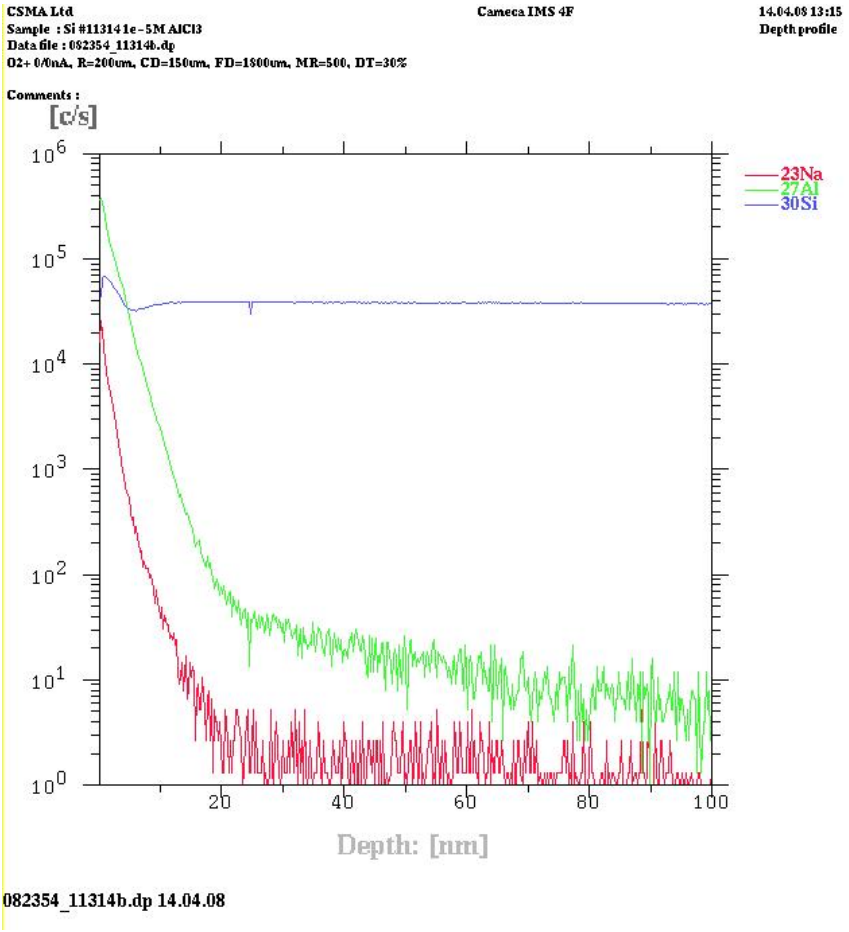

Figure 4.31 – DSIMS analysis of a plain silica wafer exposed to Aluminium Chloride. Concentration of each material is shown at increasing depth in the sample.

4.5 References

1. Grace Davison Ludox Technical Literature, P. 1-16
2. Stober W., Fink A., J. Colloid and Interface Sci. **26** (1968) 62-69
3. Tucker I., Unilever Research LPR, PS 89 6464 (1989)
4. Iler R., The Chemistry of Silica, Wiley, New York (1979)
5. Unali G., Personal Communication (2007)
6. Petkov J., Personal Communication (2007)
7. Sprycha R., J. Colloid and Interface Sci. **96** (1983) 550-554
8. Yates D.E., Levine S., Healey T.W., J. Chem. Soc. Faraday Trans.I, **70** (1974) 1807
9. Sposito G., The Environmental Chemistry of Alumina 2nd Edition, CRC Press, Florida (1996)
10. Wiese G.R., Healey T.W., J. Colloid Interface Sci. **51** (1975) 427-433
11. Tschapek M., Wasowski C., Sanchez R.M.T., J. Electroanal. Chem. **74** (1976) 167
12. Sprycha R., J. Colloid Interface Sci. **127** (1989) 1-11
13. Singh B.P., Menchavez R., Takai C., Fuji M., Takahashi M., J. Colloid Interface Sci. **291** (2005) 181-186
14. Goodwin J., Colloids and Interfaces with Surfactants and Polymers, Wiley, Sussex (2004)
15. Goodwin J., Colloids and Interfaces with Surfactants and Polymers, Wiley, Sussex (2004)
16. Szyk-Warszynska L., Trybala A., *J. Colloid Interface Sci*. **314** (2007) 398
17. Krozer A., Nordin S.A., Kasemo B., *J. Colloid Interface Sci*. **176** (1995) 479
18. Kralchevsky P. and Nagayama K. Eds, Particles at Fluid Interfaces and Membranes, Elsevier Science B.V., The Netherlands (2001)
19. Holovko M., Druchok M., Bryk T., Cation Hydrolysis Phenomenon in Aqueous Solution, Self-Organisation of Molecular Systems Series A: Chemistry and Biology, Springer (2009)
20. Thompson K., Personal Communication (2007)

5.0 Conclusions

One of the main findings (supported by different methods used) is that increasing pH causes aluminium ions to leach from the surface of the modified silica Ludox CL. The preferential adsorption of the solvated cations to anionic silica surfaces then impedes the deposition of the particles themselves. Since the leaching of aluminium ions modifies the ability of the particles to deposit on surfaces, it also changes the morphology of the particles on surfaces producing a different morphological format of aggregates.

As noted above, a variety of techniques were employed to study the dispersion and deposition of the silica particles and the reasons for the observed changes in deposition. QCM-D has been used to study adsorption of proteins[1] onto surfaces and recently at Unilever work has been performed looking at polymer adsorption[2]. Since measurement of deposition is difficult onto biological substrates, such as hair, silica wafers were chosen as a simple substrate. This meant that ellipsometry was not a reliable technique, since the refractive difference between the substrate and depositing material was very small and it was impossible to detect any deposition. QCM-D therefore seemed a suitable method to study the deposition behaviour of the silica particles onto a simple substrate. The technique is able to measure low levels of deposited material but this leads to a limited sample concentration range to stay within the linear response region of the machine. Obtaining reliable silica crystal surfaces is also essential to ensure good data. The Ludox CL material is cationic and would be expected to adhere strongly to the substrate at both the pH values studied (3 and 5). However, at pH 5, the QCM-D values decrease with increasing concentration of material. As discussed above, it appears that the aluminium coating on the Ludox particles was dissolving and releasing ions which adsorbed at the silica surface and reversed the charge. To investigate if this was the case, a dispersion of Ludox CL was placed in a dialysis bag and stirred then the diluent analysed for the presence of aluminium, showing a sharp peak in NMR assigned to Al^{3+}. Conductivity experiments were then performed on the diluent to calculate the ion concentration as amount of aluminium chloride.

A series of measurements were then performed on the silica substrate both before and after exposure to a concentration of aluminium chloride mimicking the leached

aluminium ion concentration. QCM-D was again utilised and the silica substrate was exposed to the aluminium ions. A previously deposited Ludox CL dispersion was then flowed over the crystal and no material was seen to deposit indicating the substrate surface charge was no longer negative. Streaming potential measurements were employed to determine the charge on the substrate before and after exposure to aluminium ions. Streaming potential can be difficult to measure depending upon the cell dimensions as turbulence can lead to polarisation of the electrodes and induce errors, however, the values obtained were similar to those seen previously using the same equipment[3]. The substrate was seen to carry a negative charge at pH 5 which, upon exposure to aluminium ions, resulted in charge reversal. Finally, samples of the substrate before and after exposure to aluminium ions were evaluated using DSIMS where the elements present on the surface can be identified by analysing secondary ions produced by sputtering the sample. In our case, identifying two elements on a flat substrate would be relatively straightforward and consistent data should be obtained. The silica substrate exposed to aluminium ions shows aluminium present on the surface to a depth of approximately 100nm. All these techniques indicated that exposing the substrate surface to aluminium ions would result in charge reversal and a cationic substrate. This in turn would lead to reduced deposition of the positively charged particles, seen by the QCM-D measurements and SEM images. The number of particles deposited (per cm^2) could be calculated from the mass deposited onto the QCM crystal and compared to the SEM images. However, the level of aluminium leaching from the particle coating is unknown and the leached material also deposits, therefore adding mass to the crystal.

The electrokinetic and dispersion states of the colloidal particle Ludox CL have been studied. The use of electrokinetic techniques and light scattering is commonly reported in literature and these have also been extensively developed by manufacturers to produce machines capable of consistent, robust measurements. However, to obtain meaningful data, it is essential to ensure the correct models are used and the correct descriptors for the materials as both techniques rely upon measurement due to movement of particles. In an aqueous dispersion the coated silica particles exhibit the surface properties of colloidal alumina[4] with a high cationic zeta potential at low pH values and an isoelectric point around pH 8.5-9. Aggregation of the primary particles

occurs as the pH approaches the isoelectric point due to the suppression of the electrostatic surface charges[5]. Furthermore, the primary particle size cannot recover as the pH is lowered but only irreversibly coagulated tri- and tetramer-like particle clusters are re-dispersed[6] as the electrostatic surface charges recover. This observation suggests that as aggregation takes place, counter-ion condensation leads to regions of more densely packed/aggregated primary particles which cannot be retrieved into primary particle form by recharging the alumina surface.

Aluminium oxide is a hard stable crystalline surface and therefore leaching of aluminium ions is somewhat unusual. It is therefore more likely that the oxide coating on the aluminium-coated Ludox silica is more porous than the bauxite structure and the possibilities of interplay between silica and alumina chemistry occurring is an area for future study. Initially, a comparison of the solution and deposition behaviour of the modified Ludox silica with similar sized alumina particles over a range of pH values should indicate any differences due to the silica structure. The surface of the modified silica particles could then be probed using suitable sputtering techniques.

The leaching of aluminium ions needs to be studied further as it is likely that the surface of the particles is breaking down to some degree. This may produce opportunities to control the deposition/morphology of these particles onto personal care surfaces to obtain new attributes. Further study should incorporate greater pH and electrolyte ranges of the Ludox CL dispersion with measurement of the level of leached ions in each case. The change in substrate surface charge with each level of ion leaching should be determined and the effect of this charge on deposition of Ludox CL investigated. SEM or AFM techniques could then be utilised to image and probe the morphology produced due to changes in the substrate charge.

5.1 References

1. Cans A.S., Hook F., Shupliakov O., *Analytical Chemistry* **73**, 24 (2001)
2. Webb K., PhD Thesis, Manchester University (2010)
3. Unali G., Personal Communication
4. James M., Hunter R.J., O'Brien R.W., *Langmuir* **8**, 420 (1992)
5. Wiese G.R., Healy T.W., *J Colloid Interface Sci* **51**, 3 (1975)
6. Wang X.H., Hirata Y., *J Ceramic Processing Research* **1**, 1 (2000)